Soft resummation and hard evolution

Renormalization group methods in effective theories and multi scalar models

Oredsson, Joel

2019

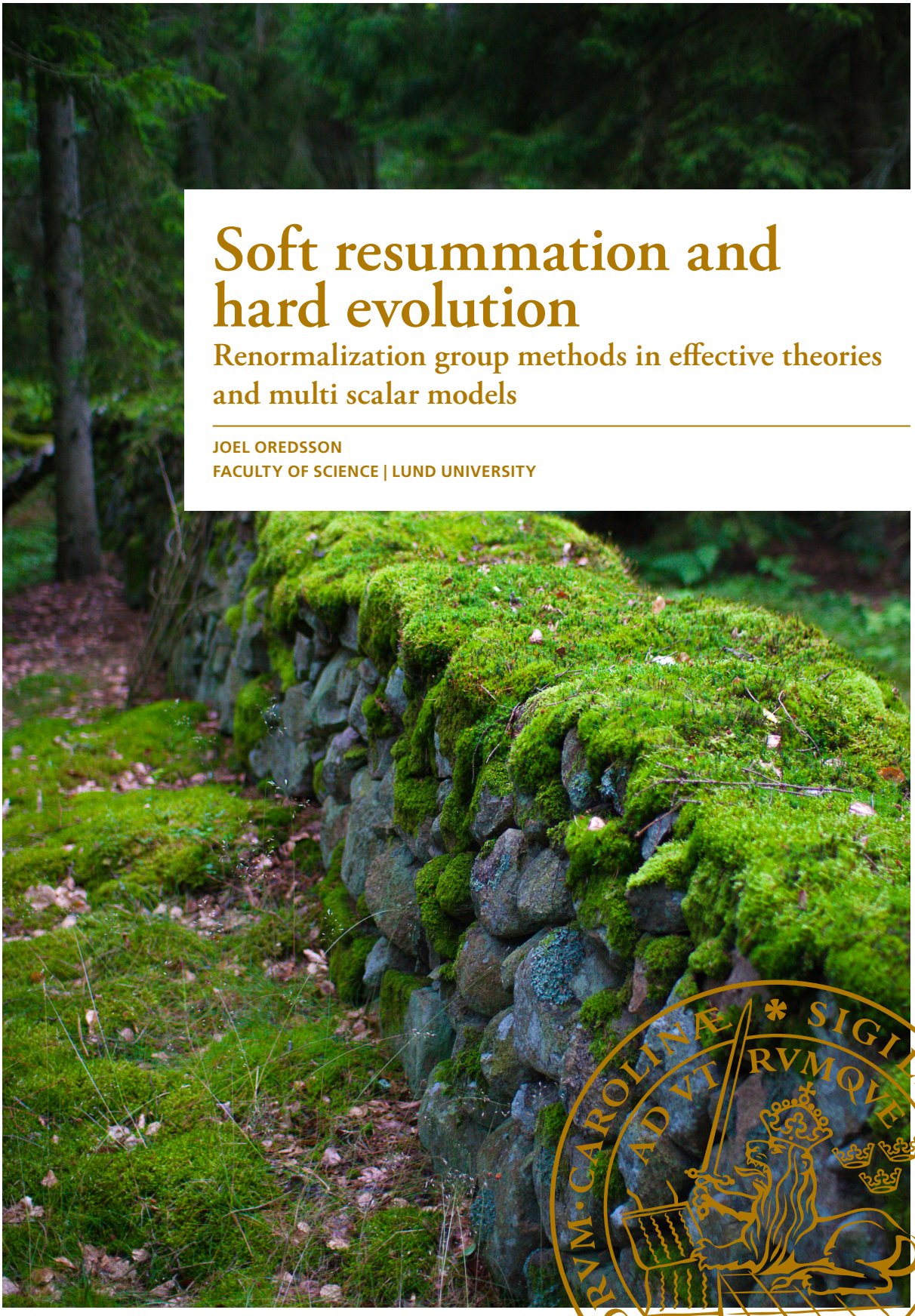

Soft resummation and hard evolution

Renormalization group methods in effective theories and multi scalar models

JOEL OREDSSON
FACULTY OF SCIENCE | LUND UNIVERSITY

Soft resummation and hard evolution

Soft resummation and hard evolution

Renormalization group methods in effective theories and multi scalar models

by Joel Oredsson

LUND
UNIVERSITY

Thesis for the degree of Doctor of Philosophy
Thesis advisors: Assoc. Prof. Johan Rathsman
Faculty opponent: Prof. Tilman Plehn

To be presented, with the permission of the Faculty of Science of Lund University, for public criticism in Rydbergsalen at the Department of Physics on Friday, the 25th of October 2019 at 10:00.

Organization
LUND UNIVERSITY

Department of Astronomy and Theoretical Physics
Sölvegatan 14A
SE–223 62 Lund
Sweden

Document name
DOCTORAL DISSERTATION

Date of disputation
2019-10-25

Sponsoring organization

Author(s)
Joel Oredsson

Title and subtitle
Soft resummation and hard evolution:Renormalization group methods in effective theories and multi scalar models

Abstract
This thesis is composed out of five papers that deal with various problems in theoretical particle physics. While paper I is a precision calculation in an effective theory of the Standard Model, papers II to V all deal with beyond the Standard Model physics. Paper IV is a manual for the tools developed during our work on papers II to V.

Paper I. We calculate the 2-loop soft function for the transverse momentum spectrum of a color-neutral final state in proton collisions in the framework of Soft-Collinear-Effective Theory. Also, the 2-loop beam functions are derived in the same framework by a comparison to other works.

Paper II. In this paper, we show that there is no need to introduce scalar kinetic mixing for models containing several identical scalar fields. This is shown by an explicit 1-loop calculation of the renormalization group equations using a toy model. The calculation is performed in separate renormalization schemes; with and without kinetic mixing. We also derive the renormalization scale dependent transformations that relate each of these schemes to one another.

Paper III. We derive the full 2-loop renormalization group equations for the general Two-Higgs-Doublet Model. With these, we analyze how a small breaking of an imposed $\mathbb{Z}_2$ symmetry spreads during renormalization group evolution in the $\mathcal{CP}$ conserving case. We perform numerical parameter scans of several physical scenarios.

Paper IV. This is a manual for the software `2HDME` that was developed to perform the numerical calculations in paper III. The code can evolve any Two-Higgs-Doublet Model at 2-loop order and perform many tree-level calculations such as masses and oblique parameters. Tests of stability and unitarity are also available.

Paper V. Here, we use `2HDME` in a similar way to paper III, but this time with the $\mathcal{CP}$ violating Two-Higgs-Doublet Model. We also implement a calculation of the electron's electric dipole moment that we use to constrain the amount of $\mathcal{CP}$ violation. We perform several numerical parameter scans of scenarios with different levels of $\mathbb{Z}_2$ symmmetry breaking.

Key words
Soft-Collinear-Effective Theory, Multi Higgs models, Two-Higgs-Doublet Model, Renormalization Group

Classification system and/or index terms (if any)

Supplementary bibliographical information

Language
English

ISSN and key title

ISBN
978-91-7895-255-7 (print)
978-91-7895-256-4 (pdf)

Recipient's notes

Number of pages
226

Price

Security classification

Signature 

Date 2019-09-13

Soft resummation and hard evolution

Renormalization group methods in effective theories and multi scalar models

by Joel Oredsson

LUND
UNIVERSITY

A doctoral thesis at a university in Sweden takes either the form of a single, cohesive research study (monograph) or a summary of research papers (compilation thesis), which the doctoral student has written alone or together with one or several other author(s).

In the latter case the thesis consists of two parts. An introductory text puts the research work into context and summarizes the main points of the papers. Then, the research publications themselves are reproduced, together with a description of the individual contributions of the authors. The research papers may either have been already published or are manuscripts at various stages (in press, submitted, or in draft).

Cover illustration front: A stone wall in Blekinge.

Cover illustration back: A boulder in Blekinge.

Faculty of Science, Department of Astronomy and Theoretical Physics

ISBN: 978-91-7895-255-7 (print)
ISBN: 978-91-7895-256-4 (pdf)

Printed in Sweden by Media-Tryck, Lund University, Lund 2019

To the absurd…

Contents

Populärvetenskaplig sammanfattning

CERN, Europas ledande laboratorium för partikelfysik, annonserade år 2012 bevis för en ny typ av partikel: higgspartikeln . Denna partikel upptäcktes i kollisioner av protoner vid Large Hadron Collider (LHC) i Geneve. Higgspartikeln är den sista pusselbiten i partikelfysikens standardmodell och experimentalister har letat efter den i decennier. Standardmodellen är en otroligt framgångsrik modell inom kvantfältsteorin och innefattar idag den elektromagnetiska kraften mellan elektroner och protoner; den starka kraften som binder samman kvarkar till protoner och neutroner; samt den svaga kraften som bland annat kopplar samman elektroner och neutriner. Higgspartikeln är speciell; dess tillhörande kvantfält ger de andra partiklarna massa genom den så kallade higgsmekanismen. I en partikelkollision sönderfaller den i princip omedelbart och man kan därför endast studera restprodukterna. Än så länge är det inte bekräftat att signalen vid LHC motsvarar standardmodellens higgspartikeln till hundra procent. Genom att mäta hur partikeln interagerar med andra partiklar så kan man säga att den liknar en standardmodell higgspartikeln, men det finns fortfarande utrymme för en mer komplicerad higgsmekanism.

Bortsett från några få undantag så stämmer standardmodellen idag överens med alla experiment gjorda vid acceleratorer på jorden. Trots detta så finns det goda indikationer för att det måste existera ny fysik; vilket skulle kräva en utökning av standardmodellen. Från astronomiska observationer så beräknas det att 85 % av universums materia måste vara i en hitintills okänd form. Denna materia reagerar ej med ljus och benämns som mörk materia. Detta är en av partikelfysikens största olösta gåtor; då ingen av partiklarna i standardmodellen passar helt in i beskrivningen. Även om de svagt växelverkande neutriner uppfyller vissa kriterier så har de för liten massa för att kunna utgöra all mörk materia.

Medan experimentallister söker efter nya partiklar i acceleratorer så jobbar teoretiker på att dels hitta på modeller för ny fysik, men också på att förbättra beräkningar av vad man förväntar sig observera i experimenten. En sådan observabel är till exempel sannolikheten för att producera en higgspartikeln vid LHC. Beräkningar inom kvantfältsteorin är dock väldigt komplicerade; kvantfluktuationer möjliggör att partiklar hela tiden skapas, transmuteras, annihileras och interagerar med varandra. Inom kvantmekaniken talar man om sannolikheter för att någonting ska ske. Dessa sannolikheter beräknas genom att summera alla kvantmekaniska amplituder; en amplitud för varje gestaltning en process kan anta. Senare i denna avhandling visualiseras sådana amplituder i form av Feynman diagram.
För att få kvantitativa resultat används ofta Monte Carlo metoder och datorkraft för att kunna simulera kvantmekaniska processer. Ett annat vanligt verktyg inom svagt växelverkande modeller är störningsteori där man kan förlita sig på enbart analytiska beräkningar. Genom att uttrycka partikelkollisioner som en summa av processer med minskande sannolikhet så kan man göra olika nivåer av approximationer; beroende på den mängd av kvantfluktuationer man tar hänsyn till.

Kvantfluktuationer har mer eller mindre betydelse beroende på vilken längdskala som undersöks. Ett exempel är vakuumpolarisation av elektronens laddning. Elektronen kan ses som en punktpartikel med ett moln av elektron-positron-par omkring sig som skapas och annihileras hela tiden. Studerar man elektronen närmare, på en mindre längdskala, så tränger man igenom detta moln som omger elektronen och elektronen växelverkar därmed starkare. Detta fenomen ger upphov till ett skalberoende för modeller inom kvantfältteorin och dess beteende vid en ändring av längdskala bestäms utav deras "*renormeringsgruppekvationer*" (RGEer).

Denna avhandlingen utgörs av arbeten såväl *inom* som *bortom* standarmodellen. Gemensamt för alla är att de fokuserar på att härleda och använda RGEer i olika modeller.

Det första projektet beräknar effekten av mjuk strålning mellan starkt växelverkande kvarkar och gluoner i en protonkollision. Denna beräkning utförs i den effektiva fältteorin "Soft-Collinear-Effective Theory". I en typisk partikelkollsion finns det en uppsjö av olika fysikfenomen vid olika längdskalor. Genom att härleda RGEer för de olika faktorer som bidrar får man en ökad precision och kontroll över osäkerheten i själva beräkningen.

Det andra projektet förklarar hur man härleder RGEer i olika ramverk för modeller som innehåller flera identiska higgsfält. Då fält med samma kvanttal blandar sig ständigt måste man systematiskt ta hänsyn till detta.

De övriga projekten sysslar alla med ett specifikt scenario: standardmodellen plus ett extra higgsfält; eller "*2-Higgs-Dublett-Modellen*" (2HDM). Detta är en populär modell att studera då bland annat teorin om supersymmetri kräver ett extra higgsfält, men 2HDM existerar också som en effektiv teori för många andra exotiska modeller. I 2HDM finns det fem stycken higgspartiklar och en utökad higgsmekanism ger ett betydligt större parameterområde. RGEer är ett effektivt verktyg för att undersöka vilken skepnad 2HDM kan ta. Genom att lösa dem ser man hur modellen beter sig vid olika längdskalor och man kan till exempel kontrollera om modellen är instabil och bryter samman vid en specifik skala. Att modellen bryter samman skulle betyda att det måste finnas ytterligare ny fysik som är relevant vid mindre skalor. I denna avhandlingens projekt härleds andra ordningens RGEer för 2HDM och programvaran, beskriven i projekt fyra, utvecklas för att kunna lösa dem numeriskt. Projekt tre och fem fokuserar på att med dessa verktyg i hand undersöka 2HDM.

List of publications

This thesis is based on the following publications:

I. **Rapidity renormalized TMD soft and beam functions at two loops**
Thomas Lübbert, Joel Oredsson and Maximilian Stahlhofen.
e-print: arXiv:1602.01829 [hep-ph]. *JHEP*, 03 (2016) 168.

II. **Scalar Kinetic Mixing and the Renormalization Group**
Johan Bijnens, Joel Oredsson, Johan Rathsman.
e-print: arXiv:1810.04483 [hep-ph]. *Phys.Lett.*, B792 (2019) 238-243.

III. **$\mathbb{Z}_2$ breaking effects in 2-loop RG evolution of 2HDM**
Joel Oredsson, Johan Rathsman.
e-print: arXiv:1810.02588 [hep-ph]. *JHEP*, 02 (2019) 152.

IV. **2 Higgs Doublet Model Evolver - Manual**
Joel Oredsson.
e-print: arXiv:1811.08215 [hep-ph]. *CPC* 2019.05.021.

V. **2-loop RG evolution of $\mathcal{CP}$ violating 2HDM**
Joel Oredsson, Johan Rathsman.
e-print: arXiv:1909.05735 [hep-ph]. *Submitted to JHEP.*

These are included in the thesis with permission from each respective publisher.

Acknowledgements

After this long of an education, I would like to thank all the wonderful teachers that I have had over the years. There are too many to count, but I have gained a lot of inspiration from many of you in Karlshamn, Lund, Santa Cruz, Hamburg and various summer schools. And there are even more that I have only learned from through books and lectures online.

Of course, I would like to thank my main supervisor Johan Rathsman for sharing his expertise with me. You have guided me through most of the research I have done here in Lund and your meticulous care for detail is impressive. I appreciate that you have given me time even when you have been very busy with other duties.

Next, I would like to thank my second supervisor Johan Bijnens for giving me many insights into both quantum field theory and general relativity. Also for straightening out our project about kinetic scalar mixing.

Many thanks to Thomas Lübbert and Maximilian Stahlhofen who collaborated with me on my first paper. You taught me many lessons about the details of writing a research paper.

Hugo Serodio should also have a special acknowledgment. I have enjoyed our many discussions about anything particle physics related; which you are always so enthusiastic about. It is too bad that our project never got finished in time to make it into my thesis, but I have learned a lot from working together.

Thanks to everyone at the department for keeping your doors open for discussions at any time and good luck to all the PhD students on their theses.

Also, thanks to Johan Rathsman and Roman Pasechnik for proofreading the introduction; there are significantly fewer typos because of you.

Lastly, I would like to thank my parents, family and friends. You have provided me with the social security to study whatever I have been interested in without hesitation. And to Annika for making the part of my life - that does not involve writing my thesis - better these past few months.

Introduction

"Confusion is a fantastic state of mind!"

Carl-Erik Magnusson

This thesis is composed out of five papers that all deal with different problems in high energy particle physics. To properly understand their content requires a working knowledge of quantum field theory. However, it is still possible to follow the broader ideas of the scientific field itself without such an expertise. A thorough introduction that is suitable for all readers is beyond the format of this thesis; as well as the capabilities of the writer. Therefore, the level of detail here starts out low, but increases dramatically.

The introduction is structured such that the first section is somewhat self-contained in that it gives a short introduction to the field of particle physics and the standard model, while at the same time also introducing the work that is presented in the papers. After the first section, the reader is assumed to be comfortable with doing tree-level calculations in quantum field theory. In section 2, the concept of the renormalization group evolution and resummation is explained by deriving the renormalization group equation for the electromagnetic charge in quantum electrodynamics. The specific *Two-Higgs-Doublet Model* that is relevant for paper III to V is presented in section 3; while the framework of paper I - *Soft-Collinear-Effective Theory* - is briefly described in section 4. After some concluding words in section 5 there is finally a compact summary of the papers and the author's contributions in section 6.

1.1. The frontier of fundamental science

Theoretical physics deals with finding the fundamental mathematical laws of nature; a quest which humankind has made great progress in. Today, we have theories that span a huge range of length scales. These agree with observations of the cosmos on galactic scales all the way down to collisions of particles in accelerators on sub-nuclear scales. There are two pillars of fundamental physics that deal with the respective ends of the probed length

scales. One is the theory of general relativity; an elegant theory that explains gravitation as things moving according to the shortest paths in four dimensional space-time. In general relativity, space-time is no longer static and flat but rather dynamical and curved by energy. The theory has been very successful in explaining, for example, the motions of the planets; time dilation effects in gravitational fields; as well as predicting the existence of gravitational waves.

The other frontier of fundamental physics is the theory of quantum fields, which is the unification of two great breakthroughs in the 20th century: the theory of special relativity and quantum mechanics. **Quantum field theory** (QFT) describes particles as excitations in their corresponding quantum fields that permeate space-time. Throughout the last approximately 100 years, physicists have found more and more particles. These were discovered in a range of different experiments. Some have been tabletop ones in small laboratories, others are studies of cosmic rays. More recently the frontier has been huge underground particle accelerators that collide particles at ever increasing energies. All these particles are collected in one model in the framework of QFT: the **Standard Model** (SM) of particle physics. This model has had unprecedented success when it comes to making precise quantitative predictions of measurements and explains essentially all earthbound high energy physics phenomenology; there are presently a few anomalies where it is currently unclear whether new physics is needed to explain the disagreement between experiments and theory.

1.2. The Standard Model of particle physics

The SM's particle content is displayed in figure 1 and can be divided into three groups:

- **Fermions** are the quarks and leptons and correspond essentially to matter particles. The familiar electron belongs to this group. Also the u and d quarks that form protons and neutrons are fermions; which together with the electron make up atoms. There are also two more generations of these mentioned fermions as well as three neutrinos.
- **Gauge bosons** refer to force carriers. The SM contains three gauge forces. One is the familiar electromagnetic force; with the photon being the gauge boson. Another is the weak force that is responsible for nuclear β-decay. Its gauge bosons are massive and are called the $W^{\pm}$ and Z bosons. The third one is the strong force that holds the quarks of the proton together with the corresponding gluons. They are massless, but, unlike the photon, they can interact with themselves.
- The last puzzle piece that was discovered in 2012 is the **Higgs boson**. It is special in that its quantum field gives masses to all the other particles through the Higgs mechanism.

Quarks:	up (2.2 MeV) down (4.7 MeV)	charm (1.3 GeV) strange (96 MeV)	top (173 GeV) bottom (4 GeV)
Leptons:	electron (0.5 MeV) ν_e (< 2.2 eV)	muon (106 MeV) ν_μ (< 0.17 MeV)	tau (1.777 GeV) ν_τ (< 18 MeV)
Vector bosons:	photon (0) Z (91 GeV)	gluon (0) $W^\pm$ (80 GeV)	
Scalar bosons:	Higgs (125 GeV)		

Figure 1: The particle content of the SM with their masses in parentheses [1]. Because of neutrino mixing, their flavor states do not have definite masses.

We can get an overview of the entire SM by writing down all the quantum fields that are present in its Lagrangian density. These are fancy words in the field of analytical mechanics, but even if one does not understand what the symbols mean - one should appreciate that it appears very compact. The structure is completely fixed by a mathematical symmetry: a so called *gauge symmetry*. After identifying the correct symmetry that gives rise to the interactions in nature, one simply writes down all of the terms that obey this symmetry. The SM can thus be written as

$$\begin{aligned}\mathcal{L} = & \underbrace{\sum_F \frac{1}{4} F_{\mu\nu} F^{\mu\nu}}_{\text{Gauge forces}} + \underbrace{\sum_\psi \bar{\psi} i \not{D} \psi}_{\text{Matter fields}} \\ & + \underbrace{(D_\mu H)^\dagger (D^\mu H) + m^2 H^\dagger H - \frac{\lambda}{4!} (H^\dagger H)^2}_{\text{Higgs field}} \\ & + \underbrace{Y_{ij} \bar{\psi}_i \psi_j H + \text{h.c.}}_{\text{Higgs-matter interactions}} \end{aligned} \tag{1}$$

and contains only about 20 parameters that need to be measured, *i.e.* they are not predicted by the theory. When those are fixed by experiments, one should in principle be able to use the SM to explain *everything* around us in our daily lives. In practice, it is highly impractical, if not impossible, to use the SM to calculate anything other than particle interactions on subatomic distances; even a single proton is immensely complicated because of the strong force that holds it together. What one does is instead to employ effective theories that contain the appropriate degrees of freedom at each length scale. Thus, to describe living organisms one would be better off using theories in psychology and neuroscience;

which, in principle, should be derivable from more fundamental sciences such as biology and chemistry. At the bottom of the inverted pyramid lies the SM.

In situations where the SM can be employed to calculate observables in experiments, the results are often impressive. One such an example of an observable that has unprecedented agreement between experiment and theory is the magnetic dipole moment of the electron. This is often parametrized in terms of $a_e \equiv (g-2)/2$, where g is a dimensionless factor that is fixed to 2 in quantum mechanics. Including quantum corrections alter this value and a_e is consequently non-zero, although very small. Recent measurements and theoretical calculations[1] give the values [2–4]

$$a_e^{\text{experiment}} = 1159652180.73(28) \times 10^{-12},$$
$$a_e^{\text{theory}} = 1159652181.643(25)(23)(16)(763) \times 10^{-12},$$

which agree to one part in 10^{-12}! The accuracy of this agreement is a great scientific achievement as well as a precision test of the SM and this is just a single example. The Particle Data Group is an international collaboration that every two years compiles a huge database of $\sim$ 40 000 [1] different measurements of the properties of elementary particles. This number should be compared to the $\sim$ 20 parameters of the SM to appreciate the SM's simplicity.

1.3. The missing pieces

Today, the SM has been tested in a wealth of different scenarios. Even though there are some anomalies that still need to be investigated, the SM largely explains all collider experiments. However, there are indications that the SM is not the full picture and that there are missing pieces. First off, the structure of the SM is very mysterious in itself in that it is not self explanatory; there are an infinite number of so called local gauge invariant QFTs that one can fill with some particle content of one's choice. Thus there are some theoretical issues that physicists try to solve by making the SM to be a mere puzzle piece in a greater mathematical structure. In the SM, the electromagnetic and weak force are unified under a single greater electroweak gauge symmetry of the theory. During the Higgs mechanism, the Higgs field acquires a vacuum expectation value which spontaneously breaks this symmetry. Afterwards, the electroweak gauge bosons mix into the massless photon as well as the massive $W^{\pm}$ and Z. The strong force is, however, independent and there are great efforts to construct *grand unification theories* that would unify all forces of the SM in a single framework.

[1] The four different theoretical uncertainties in a_e^{theory} are from perturbation theory (first two); hadronic and electroweak sectors; and the fine-structure constant respectively.

There is also another force that is totally absent in the SM: gravity. The quanta of gravity - the graviton - would have spin 2 and, for reasons that will not be covered here, no one knows how to construct such a theory that is valid on all energy scales. Thus there is a problem of quantizing gravity and unifying all the fundamental forces.

It is not only the number and types of forces that are seemingly ad-hoc in the SM. In the SM, there are three generations of fermions; the first one being the up and down quarks together with the electron and its neutrino. The second and third generation are identical to the first one, except that the particles are heavier for each step up. Also, the $\sim$ 20 free parameters in the SM exhibit some hierarchies that could be explained by an embedding of the SM in some larger framework, where the hierarchies arise from a dynamical mechanism. For example, the masses of the fermions in figure 1 vary by many orders of magnitude; even though they receive their masses from the same Higgs mechanism.

While a greater framework that could explain some of these mentioned mysterious features is desirable from a theoretical viewpoint, there are also indications of new physics that the SM cannot explain. From experiments, we know that neutrinos are massive and that they oscillate from one type to another. This can be incorporated into the SM *e.g.* by adding right-handed uncharged neutrinos.

From astronomical observations, it is now established that 85% of the matter in the universe is made up out of something other than the particles in the SM. It is electromagnetically neutral and hence dubbed dark matter. Today, there is a huge number of models beyond the SM that have a dark matter candidate in them. A popular characteristic for the candidate is that it is a weakly interacting massive particle and there is a lot of effort in searching for signals of such particles in ground based experiments.

1.4. Investigating the particle physics frontier

With the SM being so successful, it is increasingly important to test it at higher precision. Even though there are indications of the SM not being complete, there is little guidance of where to look for new physics and any disagreement of theory and data is worth investigating. Ever since its discovery, the Higgs boson has been of major interest. To see if the signal actually corresponds to the SM's Higgs boson, one must measure its interactions with itself and other particles. So far, it resembles the SM Higgs boson, but there is still room for deviations that would imply an extended scalar sector. Plenty of work is left to be done at the Higgs physics frontier; both experimentally and theoretically.

As previously mentioned, the SM is mostly used for calculations of processes at subatomic distances; such as collisions of high energy protons at the LHC. Such particle collisions are in a way very clean and simple, *e.g.* compared to the inner workings of the human

brain, but it can still be very difficult to make reliable calculations with the SM. Especially in processes that involve the strong force. Quarks and gluons carry color charge and bind together into color neutral hadrons such as the proton and it is impossible to observe a free quark. If one were to pull the quarks apart in such a hadronic state, it will be energetically favorable at a separation of about 1 fm (10^{-15} m) to produce a quark-antiquark from the vacuum so that one ends up with two hadrons instead. Thus, no matter how much force one uses, there is no way to separate the quarks in a hadron. This phenomenon is referred to as *confinement*; the quarks are confined into hadrons at large distances while behaving as, almost, free particles at sub-nuclear scales. Since the LHC is colliding hadrons, a thorough understanding of the strong force is essential in any search for new physics in such collisions.

To describe particle collisions, people often rely on computational power and Monte Carlo algorithms to simulate the scattering processes. A typical proton-proton collision exhibits multiple disparate energy scales which is a complication. Just for starters, the protons are bound objects and the hard scattering is mainly between some of its constituents. In addition to this hard process, there are soft particles with low invariant mass as well as hard jets composed out of collinear particles. Analytic calculations are possible, but require sophisticated methods of dealing with all the different phenomena in a collision. Effective field theories are employed to identify the relevant degrees of freedom and hence simplify the calculations. Recently, physicists have developed the **Soft-Collinear-Effective Theory** (SCET) framework, that, as the naming suggests, splits up the quantum fields according to the typical momenta of particles participating in a collision; excitations in collinear fields correspond to particles with collinear momenta for example. Each field then deals with a distinct region of phase space. An advantage of SCET is that it provides a clear power counting scheme at the level of the Lagrangian. This makes it possible to systematically factorize the cross section; effectively separating the hard, soft and collinear radiation into independent factors.

A specific observable that one can use SCET for is the transverse momentum spectrum of Higgs production; *i.e.* the cross section for creating a Higgs boson as a function of its momentum transverse to the beam axis. The main goal and result of paper I is the calculation of one piece of this cross section: the soft function. This function contains all the information coming from soft radiation in the scattering and can be calculated with *perturbation theory*. When using perturbation theory, one has to decide the level of radiation to include; higher levels give finer and finer approximations. Every order of approximation can be thought of as summing up all the Feynman diagrams with the number of loops being equal to the order of perturbation theory. The exact result then corresponds to summing an infinite number of diagrams ranging from having zero to an infinite number of loops. Usually one limits the calculation to zero, one or two loops; zero can be done on paper, 1-loop calculations are automatized, while 2-loop calculations are a research paper. In figure 2, a 1-loop Feynman diagram that contributes to the soft function is shown.

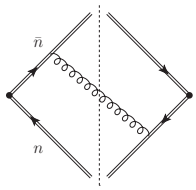

$$\propto \int \frac{\mathrm{d}^d k}{(2\pi)^d} |k^- - k^+|^{-\eta} \frac{(2\pi)\delta^+(k^2)\delta^{(2)}(\mathbf{p}_\perp - \mathbf{k}_\perp)}{k^- k^+}$$

Figure 2: The contributing Feynman diagram to the soft function at 1-loop order. The double lines represent Wilson lines and the dotted line represents the final state cut. Every cut propagator corresponds to a real emission.

By using so called **Renormalization Group Equations**[2] (RGEs) one can obtain the logarithmic contributions at every loop order. This is not simply a better approximation, but vital in certain situations where disparate energy scales produce large logarithms that spoil the convergence of perturbation theory. The process of summing up these large logarithms is referred to as *resummation*. In paper I, we calculate the soft function to 2-loop order, which produce the ingredients of next-to-next-to-leading logarithm resummation for the mentioned observable.

1.5. Going beyond the standard model

Most observables get radiative corrections when they are calculated at higher orders in perturbation theory. In an interacting quantum field theory, quantum fields are coupled together which enables particles to be created and annihilated as well as morph into each other. Even in the vacuum there are quantum fluctuations where particle and antiparticle pairs are being created and destroyed constantly. This has a *vacuum polarization* effect that can have drastic consequences for a particular model. An example is the electric charge that sets the interaction strength of the electron. The electron can be seen as a point particle that is surrounded by a cloud of virtual particle-antiparticle pairs that make the vacuum behave as a dielectric medium. These pairs are effectively dipoles that screen the true charge, as illustrated in figure 3. When probing the electron at smaller length scales, the electromagnetic interaction strength grows as one penetrates the cloud of virtual particles. This effect will be discussed in greater detail in section 2, where we derive the RGE for the electromagnetic interaction strength in quantum electrodynamics.

The energy dependence of quantum fluctuations is governed by the previously mentioned

[2]Such renormalization group equations are essential for this thesis and are described in more detail in the following sections.

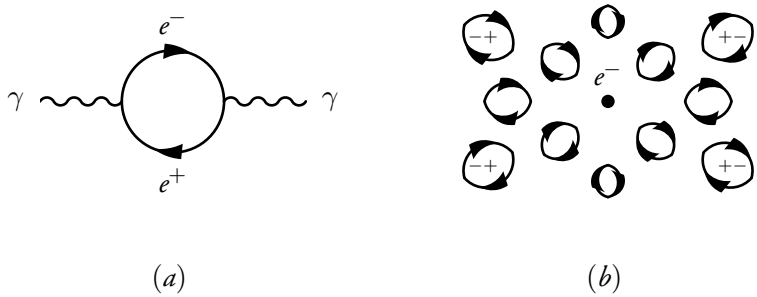

Figure 3: (a): Feynman diagram that leads to the vacuum polarization of the electromagnetic field. (b): Radiative corrections cause the vacuum to behave like a dielectric medium. The charge of the electron is shielded by a cloud of virtual electron-positron pairs, which consequentially leads to one measuring a stronger electromagnetic interaction at smaller distances.

RGEs. By solving them, one performs a resummation of large logarithms and achieves predictability in regions where fixed order perturbation theory breaks down. When analyzing models beyond the SM, this is a very powerful tool. Using these equations, one can extrapolate models to energy regimes well outside of the available experimental reach.

Papers III to V, deal with a specific model beyond the SM: the **Two-Higgs-Doublet Model** (2HDM). This model is a minimalistic extension of the SM; it simply adds an additional Higgs field to the scalar sector. There are many motivations for investigating the 2HDM that make it one of the most studied model beyond the SM. Perhaps the biggest motivation comes from low energy supersymmetry; which requires two Higgs fields to be mathematically consistent. But it is also interesting to study a non-minimal scalar sector in its own right; much like there are interesting consequences from having non-minimal fermion sector with multiple fermion generations in the SM.

The 2HDM has a rich scalar phenomenology sector with three neutral and one charged pair of Higgs bosons. While the experimental community searches for new scalar particles using colliders, there is plenty of work for the theorists to do. To guide the experiments and for its own interest, one can investigate the parameter space of the 2HDM using all the theoretical tools available. The RGEs that govern the model's energy dependence contain a wealth of information. By solving them, one can probe the models behavior at different length scales. One of the goals of this thesis is therefore to investigate the behavior of different scenarios for the 2HDM under renormalization group evolution.

One of the main subject of paper III is the derivation and usage of the 2-loop RGEs for the general 2HDM. The 2-loop RGEs for a general renormalizable QFT in four dimensions are

known [5–8]. However, there are some subtleties when working with models that exhibit multiple identical scalar fields and the results of refs. [5–8] need some careful generalization. Paper II describes how one can construct different renormalization schemes that handle this case. The paper is not specifically about the 2HDM, but focuses on models that exhibit multiple identical scalar fields.

While paper III deals with the $\mathcal{CP}$ conserving 2HDM, paper V completes the analysis by also investigating $\mathcal{CP}$ violation effects. During this work we developed the open-source software `2HDME` that, among other things, can solve the RGEs for 2HDM numerically. Paper IV is a manual for this code.

2. Quantum fluctuations

All the papers of this thesis deal with RGEs in one way or the other. These equations are a powerful tool to investigate new physics models, as well as resumming large logarithms in calculations of observables at colliders. Since they are of such importance, we will in this section go through where they come from in more detail.

As a first investigation of the renormalization group, we will study the familiar force of electrodynamics; more specifically, we will calculate the effect on the strength of electromagnetic interactions from quantum fluctuations. The interactions of electrons, positrons and photons are all governed by the theory of quantum electrodynamics; with the basic $U(1)_{em}$ gauge invariant Lagrangian

$$\mathcal{L} = \frac{1}{4}F_{\mu\nu}F^{\mu\nu} + \bar{\psi}(i\partial\!\!\!/ + e_b A\!\!\!/ - m)\psi. \tag{2}$$

This describes most of the everyday macroscopic phenomena, in principle, with only two free parameters: the electron mass, $m \approx 0.5$ MeV, and the electromagnetic charge[3], e_b. It is worth emphasizing that the parameters of the Lagrangian do *not* correspond directly to observables and one must in general employ a renormalization scheme when performing loop calculations in QFT. The whole procedure of renormalization is essentially the process of relating physical observables to other observables. Therefore, we will begin by investigating one such familiar measurable quantity: the Coulomb force.

2.1. The Coulomb potential

The charge sets the strength of the electromagnetic interactions between two particles. At macroscopic distances it should reduce to the Coulomb force, which we will first derive.

[3]In this section we only denote the bare electromagnetic charge with a subscript b in order not to clutter the formulas. In reality, the mass will also get radiative corrections and hence should also be renormalized.

The system we will investigate is that of two static sources that we label as

$$J_a^\mu(\vec{x}) : \begin{cases} J_a^0(\vec{x}) = e_b \delta^{(3)}(\vec{x} - \vec{x}_a), \\ J_a^i(\vec{x}) = 0. \end{cases} \qquad J_a^\mu(\vec{q}) : \begin{cases} J_a^0(\vec{q}) = e_b e^{-i\vec{q}\cdot\vec{x}_a}, \\ J_a^i(\vec{q}) = 0. \end{cases} \tag{3}$$

for $a = 1, 2$ in position and momentum space respectively. To get to the Coulomb force, we start off with the energy functional $E[J] = -i \log Z[J]$, where $Z[J]$ is

$$Z[J] = \int \mathcal{D}\bar{\psi}\mathcal{D}\psi\mathcal{D}A \exp\left[i \int \mathrm{d}^4x \mathcal{L} + J^\mu A_\mu \right]. \tag{4}$$

The energy functional is a generating functional for connected Green functions,

$$\frac{\delta E}{\delta J^\mu \delta J^\nu} = -iD_{\mu\nu} = \langle \Omega | \, T\{A_\mu A_\nu\} \, | \Omega \rangle_{\text{connected}} . \tag{5}$$

It can thus be expressed as

$$E[J] = -\frac{i}{2} \int \frac{\mathrm{d}^4 q}{(2\pi)^4} J^\mu(\vec{q})^* D_{\mu\nu}(q^2) J^\nu(\vec{q}), \tag{6}$$

where J denotes the sum of all currents. Plugging in the currents in eq. (3), it becomes a function of $\vec{r} = \vec{x}_1 - \vec{x}_2$,

$$E(\vec{r}) = -ie_b^2 \int \frac{\mathrm{d}^4 q}{(2\pi)^4} e^{-iq\cdot r} D_{00}(q^2) + (r \text{ independent terms}). \tag{7}$$

Since it gives the energy in the system as a functional of the sources, we identify the Coulomb potential as the r-dependent term. In momentum space, we arrive at the simple expression for the Coulomb potential:

$$\tilde{V}(q^2) = ie_b^2 D_{00}(q^2). \tag{8}$$

To proceed, we need to compute the 2-point correlation function: the propagator. The photon propagator can be written as a series of connecting **1-Particle Irreducible** (1PI) diagrams,

$$i\Pi^{\mu\nu}(q^2) \equiv \mu \sim\!\!\textcircled{\text{1PI}}\!\!\sim \nu \equiv i(q^2 g^{\mu\nu} - q^\mu q^\nu)\Pi(q^2), \tag{9}$$

where the tensor structure follows from Lorentz invariance. The full propagator form a geometric series that can be summed up to give

$$\begin{aligned} D_{\mu\nu}(q^2) &= \mu \sim\sim \nu + \mu \sim\!\!\textcircled{\text{1PI}}\!\!\sim \nu + \mu \sim\!\!\textcircled{\text{1PI}}\!\!\textcircled{\text{1PI}}\!\!\sim \nu + \ldots \\ &= \frac{-i}{q^2[1 - \Pi(q^2)]} \left(g_{\mu\nu} - \frac{q_\mu q_\nu}{q^2} \right) + \frac{-i}{q^2} \left(\frac{q_\mu q_\nu}{q^2} \right). \end{aligned} \tag{10}$$

The terms proportional to momentum components are in fact gauge dependent and we can omit them from here on for our computation.

To 1-loop order, we define $\Pi(q^2) = \Pi_2(q^2) + \mathcal{O}\left(e_b^4\right)$ which corresponds to the Feynman diagram

$$i\Pi_2^{\mu\nu}(q^2) \equiv \mu \sim\!\bigcirc\!\sim \nu = i(q^2 g^{\mu\nu} - q^\mu q^\nu)\Pi_2(q^2)$$

$$= -e_b^2 \mu^{4-d} \int \frac{\mathrm{d}^d k}{(2\pi)^d} \frac{\mathrm{Tr}\left[\gamma^\mu(\not{k} + m)\gamma^\nu(\not{k} + \not{q} + m)\right]}{(k^2 - m^2)\left[(k+q)^2 - m^2\right]}. \tag{11}$$

Here, we use dimensional regularization in $d = 4 - 2\epsilon$ dimensions and μ is a renormalization scale that is introduced for dimensional reasons; it will cancel out in all physical observables. In the high energy limit, $-q^2 \gg m^2$, a straightforward calculation gives

$$\Pi_2(-q^2 = Q^2) = -\frac{e_b^2}{12\pi^2}\left[\frac{1}{\epsilon} + \frac{5}{3} + \log\left(\mu^2/Q^2\right)\right] + \mathcal{O}\left(m^2/Q^2\right). \tag{12}$$

With the results from the 1-loop computation of the propagator, the Coulomb potential in momentum space is

$$\tilde{V}(q^2) = \frac{e_b^2}{q^2\left[1 - \Pi_2(q^2)\right]}. \tag{13}$$

Now, we have an expression for the Coulomb potential in terms of the bare electromagnetic charge. One must now define the electromagnetic coupling in the Lagrangian through some *renormalization condition*; that relates it to something measurable. A natural choice here is to define it so that the Coulomb potential at some reference scale Q_0^2, or r_0, reduces to the ordinary classical result $V(r_0) = e(r_0)^2/(4\pi r_0)$ in position space and $\tilde{V}(Q_0^2) = e(Q_0)^2/Q_0^2$ in momentum space. The parameter $e(Q_0)$ is then a measurable quantity that we have an expression for from the above 1-loop calculation,

$$e(Q_0)^2 \equiv e_b^2\left[1 + \Pi_2(Q_0^2)\right] + \mathcal{O}\left(e_b^6\right). \tag{14}$$

This is so far not a very useful formula. If the right hand side of eq. (14) actually was known, it would be incredible since we then could calculate the fine structure constant from first principles. Sadly this is not so since we do not know e_b and furthermore $\Pi_2(Q_0^2)$ contains $1/\epsilon$ poles and the unphysical renormalization scale μ. However, what we *can* compute is the coupling strength $e(Q)$ at another energy scale by relating it to the measured $e(Q_0)$. By iteratively solving $e(Q)$ in terms of $e(Q_0)$ with eq. (14), we end up with the result

$$\begin{aligned} e(Q)^2 &= e(Q_0)^2\left\{1 + \left[\Pi(Q^2) - \Pi(Q_0^2)\right]\right\} + \mathcal{O}[e(Q_0)^6] \\ &= e(Q_0)^2\left[1 + \frac{e(Q_0)^2}{12\pi^2}\log\left(Q^2/Q_0^2\right)\right] + \mathcal{O}[e(Q_0)^6]. \end{aligned} \tag{15}$$

This definition of the coupling parameter is often referred to as a *running coupling* since it depends on the energy scale of the physical process at which it is used to calculate observables. It actually grows logarithmically as one goes to higher energies; equivalently, smaller distances.

2.2. Large logarithms calls for resummation

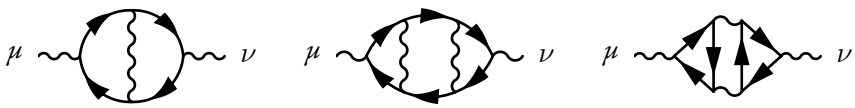

Figure 4: Examples of higher order loop corrections to the vacuum polarization in quantum electrodynamics.

With eq. (15), we can compute e at another energy scale. However, we only calculated the 1-loop diagram; at higher loop levels there are additional diagrams like the ones in figure 4. Denoting $e(Q) \equiv e$, $e(Q_0) \equiv e_0$ and $\log(Q^2/Q_0^2) \equiv L$, we can sketch what the result would be to higher orders

$$\begin{aligned} e^2 \sim e_0^2 + e_0^4 L + e_0^6 L^2 + e_0^8 L^3 + \dots \text{ (LL)} \\ + e_0^4 \quad + e_0^6 L \quad + e_0^8 L^2 + \dots \text{ (NLL)} \\ + e_0^6 \quad + e_0^8 L \quad + \dots \text{ (NNLL)}, \end{aligned} \tag{16}$$

where we have grouped the perturbation series in powers of e_0 as well as powers of L. When e_0 and L are much smaller than 1, the first few terms should be sufficient to get a reliable prediction of e. There is a problem though if one deals with disparate energy scales. If $L \sim 1/e_0$, large logarithms spoil the convergence of perturbation theory since the first row contains $\mathcal{O}(1)$ terms[4]. There is however an easy way to sum up all of these terms that contain logarithms. Summing up the first row is referred to as Leading-Log (LL) resummation; including the logarithmic terms in the second row would correspond to Next-to-LL (NLL) and so on. We know the energy dependence of $e(Q)$ from eq. (15) and by taking the derivative with respect to $\log(Q)$ we end up with

$$\beta_e \equiv \frac{\mathrm{d}}{\mathrm{d}\log Q} e(Q) = \frac{e(Q)^3}{12\pi^2}. \tag{17}$$

This is an example of a RGE that was mentioned in the introduction. The RGE for the running coupling $e(Q)$ is also referred to as the coupling's beta function. Equations such as this

[4]This is more often the case when one deals with the strong force because of the large α_s coupling.

one governs the energy dependence of theories and a tremendous amount of information about the theory can be said by analyzing it.

In this simple case where there is just a single RGE with one variable, one can solve eq. (17) analytically, which gives the electromagnetic charge at one scale in terms of it at another scale,

$$e(Q) = \frac{e(Q_0)}{\sqrt{1 - \frac{e(Q_0)^2}{12\pi^2} \log\left(Q^2/Q_0^2\right)}}. \tag{18}$$

This corresponds to the LL resummation as can be seen if one Taylor expands eq. (18) and compares with eq. (16).

To summarize, we have defined a parameter $e(Q_0)$, that is fixed to some measured value at a particular energy scale Q_0; where the experiment is performed. Then we used perturbation theory to calculate this parameter at a different scale Q. Furthermore, this leads to a differential equation that can be integrated, which yields the running coupling $e(Q)$. The renormalization scale Q should be chosen to be the characteristic energy scale of the process under consideration in calculations of cross sections and decay rates.

2.3. Renormalization group evolution

Since $e(Q)$ is the only parameter in the Lagrangian of quantum electrodynamics, except the electron mass, we have all the ingredients necessary to investigate how the theory behaves at length scales that have not yet been probed experimentally. When we renormalized the electric charge, we defined it so that quantum electrodynamics reduces to the Coulomb law at large distances; where the charge $e(Q)$ gets no radiative corrections by definition. Since β_e in eq. (17) is positive, the electromagnetic strength grows when performing experiments at higher energies; or equivalently smaller distances. That the charge grows as one probes the electron at smaller scales was already mentioned in section 1.5 and is physically illustrated in figure 3. There, the electron is seen as a point particle surrounded by a cloud of virtual e^-e^+ pairs that shield the bare charge and consequently make the vacuum behave like a dielectric medium.

Even though one now can extrapolate $e(Q)$ to very large energies, at one point $e(Q)$ will become too large and we loose any predictability since perturbation theory then breaks down. In quantum electrodynamics, this scale is however enormous and way beyond any energy scale that is experimentally interesting. The *Landau pole* is defined as the singularity where $e(Q)$ goes to infinity, *i.e* where the denominator of eq. (18) is zero,

$$\Lambda_{\text{Landau}} = m_e \exp\left[6\pi^2/e(m_e)^2\right] \approx 10^{286}\ \text{eV}. \tag{19}$$

Its presence is a sign that the theory becomes strongly coupled or is incomplete and new physics should enter at some energy scale below Λ_{Landau}.

Another characteristic behavior under renormalization group evolution is exhibited in the SM. The strong interaction strength of quarks and gluons is fixed by the $SU(3)_c$ coupling g_3, with the 1-loop beta function[5]

$$\beta_{g_3} = -\frac{7g_3^3}{16\pi^2}. \tag{20}$$

That the sign of β_{g_3} is negative is of crucial importance; it means that the strong interaction is only strongly coupled at large distances. The Landau pole $\Lambda_{\text{QCD}} \approx 200$ MeV gives the energy scale where this occurs. This corresponds to a distance $1/\Lambda_{\text{QCD}} \sim 10^{-15}$ m, which is roughly the size of light hadrons. Below that scale, one has to resort to some effective theory or non-perturbative lattice computations to make predictions. At the opposite end, one can use perturbation theory at energies above $\mu \sim 1$ GeV. The quarks and gluons are thus weakly coupled when going to smaller distance; a phenomenon known as asymptotic freedom. In figure 5 all the gauge couplings in the SM are plotted as functions of the renormalization scale.

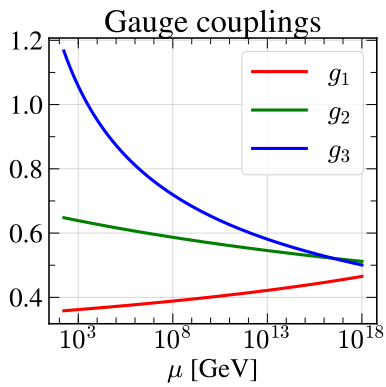

Figure 5: The running gauge couplings $g_{1,2,3}$ for the SM's gauge groups $U(1)_Y$, $SU(2)_W$ and $SU(3)_c$ respectively as functions of the renormalization scale. The running is performed at 2-loop order with the default SM class in `2HDME` [9].

By studying the RGEs of a theory, one can extrapolate its behavior to energies that have not yet been probed experimentally. In this way, it is a powerful tool when investigating new models in QFT; their behavior under the RG evolution tells us the models' energy range of validity. If the RG evolution is very sensitive to the choice of parameters at one scale,

[5]The beta function for g_3 actually depends on the number of active quark flavors, which itself depends on the energy scale. The given β_{g_3} is valid for six quark flavors.

it would be sign that the model is either fine-tuned or unstable. A Landau pole is a clear indication that a model breaks down, but one can also investigate other features as well. Any inconsistency gives valuable information about the model under consideration.

2.4. Renormalization group: the general picture

In the previous section we saw examples of running couplings with an energy dependence governed by their respective RGE. Here, we sketch the general process of renormalization that gives a system of such equations.

As explained in the beginning of this section, one needs to match the parameters in the Lagrangian to physical observables with some renormalization scheme when calculating something in quantum field theory. Each parameter will be fixed at a certain energy scale by a renormalization condition. The choice of renormalization scale is completely arbitrary; physical observables do not care at which scale you define your parameters.

Say we have a simple theory consisting of a single scalar field,

$$\mathcal{L} = \frac{1}{2}(\partial\phi_b)^2 - \frac{1}{2}m_b^2\phi_b^2 - \frac{\lambda_b}{4!}\phi_b^4, \tag{21}$$

where we now have written all bare (unrenormalized) quantities with a subscript b. All bare parameters in the Lagrangian can be factorized into a renormalization factor, Z, and a renormalized running coupling/field, like

$$\phi_b = Z(\mu)\phi(\mu), \qquad \lambda_b = \mu^{2\epsilon}Z_\lambda(\mu)\lambda(\mu), \tag{22}$$

where the $\mu^{2\epsilon}$ factor is inserted to make the renormalized coupling dimensionless[6]. The renormalization scale μ will play the same role as the scale Q in section 2. Any object that is expressed with bare quantities is of course μ-independent. This, almost trivial, statement is used when deriving the RGEs for renormalized quantities.

If we for example look at the bare n-point correlation function, which will depend on the bare Lagrangian parameters, it is related to the renormalized n-point function as

$$G_b^{(n)}(\{x_i\}, m_b, \lambda_b) = Z(\mu)^{n/2}G^{(n)}(\{x_i\}, m(\mu), \lambda(\mu), \mu). \tag{23}$$

Since the LHS does not depend on μ, we take the derivative with respect to μ, which gives

$$0 = \mu\frac{\mathrm{d}}{\mathrm{d}\mu}G_b = \frac{n}{2}Z^{\frac{n}{2}-1}\left(\mu\frac{\mathrm{d}}{\mathrm{d}\mu}Z\right)G^{(n)} + Z^{n/2}\mu\frac{\mathrm{d}}{\mathrm{d}\mu}G^{(n)}. \tag{24}$$

[6]In dimensional regularization, the dimensionless action is $\int \mathrm{d}^dx\mathcal{L}$ which changes the dimensionality of the fields; from $[\mathcal{L}] = d$, one derives $[\phi] = (d-2)/2 = 1-\epsilon$.

If we rearrange this equation, we arrive at the so called *Callan-Symanzik* equation,

$$\left[\mu\frac{\partial}{\partial\mu}+\beta_m\frac{\partial}{\partial m}+\beta_\lambda\frac{\partial}{\partial\lambda}+\frac{n}{2}\gamma\right]G^{(n)}(\{x_i\},m(\mu),\lambda(\mu),\mu)=0, \tag{25}$$

where we have defined the beta functions for the running parameters,

$$\beta_\lambda\equiv\mu\frac{\mathrm{d}}{\mathrm{d}\mu}\lambda(\mu), \qquad\qquad \beta_m\equiv\mu\frac{\mathrm{d}}{\mathrm{d}\mu}m(\mu). \tag{26}$$

The corresponding beta function for the scalar fields in eq. (25) is referred to as the anomalous dimension, which is similarly defined as

$$\mu\frac{\mathrm{d}}{\mathrm{d}\mu}\phi(\mu)\equiv\gamma\phi(\mu). \tag{27}$$

In the end, all renormalized parameters have their own RGE. We have previously seen examples of the RGEs of gauge couplings to 1-loop order that only depend on the gauge coupling itself. In such scenarios it is easy to solve the RGEs analytically like in eq. (18). The Yukawa sector and scalar potential RGEs are in general more complicated and all the RGEs form a system of coupled ordinary differential equations. Thus, one needs to rely on numerical solutions when performing the RG evolution.

3. Two-Higgs-Doublet Model

"I'm Mr.Meeseeks! Look at me!"

Mr.Meeseeks, Rick and Morty

While the gauge and fermion sectors of the SM are by now well established, the scalar sector has just, in recent years, begun to be probed phenomenologically. Contrary to the fermion sector, with its multiple families and mixings, which is seemingly more complicated than necessary without any apparent reason, the scalar sector of the SM is minimalistic with a single $SU(2)$ doublet.

Although the 125 GeV scalar particle at the LHC [10, 11] so far resembles the SM's Higgs boson [12], its true nature is not yet fully explored. There is still room for an extended and more complicated scalar sector; it is not hard to imagine a bigger scalar sector with the minimal choice existing as a limit of it.

There is, however, one parameter that severely constrains the choice of scalar fields to use for a $SU(2)_W \times U(1)_Y$ gauge theory. At tree-level this parameter is [13]

$$\rho = \frac{\sum_i \left[I_i(I_i+1) - Y_i^2/4 \right] v_i}{\sum_i Y_i^2 v_i/2}, \tag{28}$$

where the I_i, Y_i and v_i are the weak isospin, hypercharge and **Vacuum Expectation Value** (VEV) respectively, for all the scalar multiplets labeled by the index i in the theory. Experimentally, this parameter is measured to be $\rho = 1.00039 \pm 0.00019$ [1]; in agreement with the SM's prediction, $\rho = 1$. This can be used to constrain higher dimensional representations of scalar fields; though, all extensions with doublets that have $I_i = 1/2$ and $Y_i = \pm 1$ preserve $\rho = 1$. The minimal choice of adding one extra scalar doublet to the SM gives the 2HDM [14]. It is thus one of the simplest extensions of the SM's scalar sector.

Even though the addition of a *single* Higgs doublet might seem like a small change, the consequences can be drastic. In the SM, going from two to three fermion families opens up for $\mathcal{CP}$ violation in the Yukawa sector by having a phase in the CKM matrix after diagonalizing the Yukawa matrices. In the 2HDM there are many more Yukawa couplings that are potentially complex even after going to the fermion mass basis. Similarly, the 2HDM exhibits the possibility of explicit as well as spontaneous $\mathcal{CP}$ violation in the scalar potential [14]. These new sources of $\mathcal{CP}$ violation make up an attractive feature of the 2HDM and was the motivation for studying the 2HDM in the first place [14].

There are other motivations for choosing to study the 2HDM in addition to investigating a non-minimalistic theory. Perhaps the greatest motivation comes from low-energy *supersymmetry* [15, 16]. In the *minimal supersymmetric SM*, the scalar fields belong to chiral

multiplets while their complex conjugates are in a multiplet of opposite chirality; hence, a single scalar field cannot give masses to both up and down type quarks. Because of this reason, supersymmetry requires at least two Higgs doublets; it also solves the problem of cancelling anomalies in the minimal supersymmetric SM.

Many non-supersymmetric models beyond the SM also exhibit two Higgs doublets. For example, the *Peccei-Quinn mechanism* [17] in axion models requires two Higgs doublets making the 2HDM into a low-energy effective theory [18].

Given the popularity of the 2HDM, there is a huge amount of work that has been done in the literature. For more details, see the review in ref. [19].

3.1. The Standard Model revisited

The content of the SM was briefly covered in section 1.2. Here, we will revisit it with more details to prepare for the 2HDM. The SM is a $SU(3)_c \times SU(2)_W \times U(1)_Y$ gauge theory that is spontaneously broken down to $SU(3)_c \times U(1)_{\text{em}}$. Its potential and Yukawa sectors are

$$V_{\text{SM}} = m_{11}^2 \Phi_1^\dagger \Phi_1 + \frac{1}{2}\lambda_1 \left(\Phi_1^\dagger \Phi_1\right)^2 \tag{29}$$

and

$$\mathcal{L}_{\text{SM}}^Y = -\bar{Q}_L \cdot \tilde{\Phi}_1 \eta_1^U U_R - \bar{Q}_L \cdot \Phi_1 \eta_1^{D\dagger} D_R - \bar{L}_L \cdot \Phi_1 \eta_1^{L\dagger} E_R + \text{h.c.} \tag{30}$$

respectively, where $\tilde{\Phi}_i \equiv i\sigma_2 \Phi_i^*$ and the left-handed fermion fields are

$$Q_L \equiv \begin{pmatrix} U_L \\ D_L \end{pmatrix}, \qquad L_L \equiv \begin{pmatrix} \nu_L \\ E_L \end{pmatrix}. \tag{31}$$

The 3-by-3 η_1^F matrices are the Yukawa couplings in the fermion flavor space. These will be diagonalized when going to the fermion mass-eigenstate basis. The Φ_1 field is a $SU(2)_W$ doublet that acquires a vacuum expectation value, v, during the Higgs mechanism. With a gauge transformation, it can be brought into the form

$$\Phi_1 = \frac{1}{\sqrt{2}} \begin{pmatrix} \sqrt{2}G^+ \\ v + h(x) + iG^0 \end{pmatrix}. \tag{32}$$

Of the four degrees of freedom of the Higgs field, the three $G^{+,0}$ are "eaten" by $W^\pm$ and Z while one corresponds to a physical Higgs boson, $h(x)$, with the masses

$$m_{W^\pm} = vg/2, \qquad m_Z = v\sqrt{g^2 + g'^2}/2, \qquad m_h = v\sqrt{\lambda_1}, \tag{33}$$

where g and g' denote the gauge couplings of $SU(2)_W$ and $U(1)_Y$ respectively.

Imposing that the ground state is in a minimum of the potential gives the relation $v = \sqrt{-2m_{11}^2/\lambda_1}$, which removes one of the three free parameters. If one fixes $v = 1/\sqrt{G_F} \approx 246$ GeV, one is left with a single parameter that is fixed by the mass of the Higgs boson.

So far the minimal scalar sector of the SM is sufficient to explain the phenomenology at the current colliders. However, not all interactions have been probed experimentally. One interaction that will be of paramount importance is the triple Higgs boson interaction vertex that is predicted to

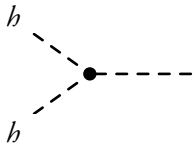

$$= -3i\frac{m_h^2}{v}. \tag{34}$$

Measuring this interaction will be a rigorous test of the structure of the electroweak symmetry breaking. It is, however, not an easy experiment to perform; the best channel is through double Higgs production. This is therefore left as a challenge for future colliders [20].

3.2. Adding a doublet

The 2HDM simply extends the scalar sector of the SM with an additional scalar doublet, Φ_2. This results in the potential

$$\begin{aligned} V_{\text{2HDM}} =& m_{11}^2\Phi_1^\dagger\Phi_1 + m_{22}^2\Phi_2^\dagger\Phi_2 - (m_{12}^2\Phi_1^\dagger\Phi_2 + \text{h.c.}) + \frac{1}{2}\lambda_1\left(\Phi_1^\dagger\Phi_1\right)^2 + \frac{1}{2}\lambda_2\left(\Phi_2^\dagger\Phi_2\right)^2 \\ &+ \lambda_3\left(\Phi_1^\dagger\Phi_1\right)\left(\Phi_2^\dagger\Phi_2\right) + \lambda_4\left(\Phi_1^\dagger\Phi_2\right)\left(\Phi_2^\dagger\Phi_1\right) \\ &+ \left[\frac{1}{2}\lambda_5\left(\Phi_1^\dagger\Phi_2\right)^2 + \lambda_6\left(\Phi_1^\dagger\Phi_1\right)\left(\Phi_1^\dagger\Phi_2\right) + \lambda_7\left(\Phi_2^\dagger\Phi_2\right)\left(\Phi_1^\dagger\Phi_2\right) + \text{h.c.}\right]. \end{aligned} \tag{35}$$

In general, the parameters m_{12}^2 and $\lambda_{5,6,7}$ are complex. The potential then exhibits 14 degrees of freedom. Out of these, three are removed by the tadpole equations while one can be removed by a re-phasing of one of the Higgs fields.

After a gauge transformation, the Higgs fields' VEVs acquire the forms[7]

$$\langle\Phi_1\rangle = \frac{v}{\sqrt{2}}\begin{pmatrix} 0 \\ c_\beta \end{pmatrix}, \qquad \langle\Phi_2\rangle = \frac{v}{\sqrt{2}}\begin{pmatrix} 0 \\ s_\beta e^{i\xi} \end{pmatrix}. \tag{36}$$

[7] c_β (s_β) is short notation for $\cos\beta$ ($\sin\beta$).

There are different *Higgs flavor bases* that all are related by $U(2)$ field redefinitions that leave the kinetic terms invariant. This implies that only invariant quantities under such a transformation in the 2HDM can correspond to something physical and it is therefore convenient to use the Higgs flavor base-independent methods of refs. [21–23]. We mostly employ their notation in the following.

The *Higgs basis* [21, 24] is one particular convenient basis; in it, only one Higgs field gets a VEV. By defining the transformation matrix

$$\hat{U} = \begin{pmatrix} \hat{v}_1^* & \hat{v}_2^* \\ \hat{w}_1^* & \hat{w}_2^* \end{pmatrix} = \begin{pmatrix} c_\beta & e^{-i\xi} s_\beta \\ -e^{i\xi} s_\beta & c_\beta \end{pmatrix}, \tag{37}$$

one can express the Higgs fields in the Higgs basis in terms of the fields in the *generic basis* as $H_a = \hat{U}_{a\bar{b}} \Phi_b$, with the inverse $\Phi_a = \hat{U}^\dagger_{a\bar{b}} H_b$. These fields take the form

$$H_1 = \begin{pmatrix} G^\pm \\ \frac{1}{\sqrt{2}}(v + \varphi_1 + iG^0) \end{pmatrix}, \qquad H_2 = \begin{pmatrix} H^\pm \\ \frac{1}{\sqrt{2}}(\varphi_2 + ia_0) \end{pmatrix}. \tag{38}$$

After electroweak symmetry breaking, the $G^\pm$ and G^0 are the Goldstone bosons that are eaten by the $W^\pm$ and Z. The $H^\pm$ is a charged scalar field, while $\varphi_{1,2}$ and a_0 all mix into three neutral Higgs particles, h_k; of indefinite $\mathcal{CP}$ properties if the scalar potential exhibits $\mathcal{CP}$ violation. The scalar potential in the Higgs basis is of the same form as in the generic basis,

$$\begin{aligned} -\mathcal{L}_V = {} & Y_1 H_1^\dagger H_1 + Y_2 H_2^\dagger H_2 + \Big(Y_3 H_1^\dagger H_2 + \text{h.c.} \Big) + \frac{1}{2} Z_1 (H_1^\dagger H_1)^2 + \frac{1}{2} Z_2 (H_2^\dagger H_2)^2 \\ & + \frac{1}{2} Z_3 (H_1^\dagger H_1)(H_2^\dagger H_2) + \frac{1}{2} Z_4 (H_1^\dagger H_2)(H_2^\dagger H_1) \\ & + \left\{ \frac{1}{2} Z_5 (H_1^\dagger H_2)^2 + \Big[Z_6 (H_1^\dagger H_1) + Z_7 (H_2^\dagger H_2) \Big] H_1^\dagger H_2 + \text{h.c.} \right\} .. \end{aligned} \tag{39}$$

The Yukawa sector is, in the generic basis,

$$\mathcal{L}^Y_{\text{2HDM}} = \sum_{i=1}^{2} \Big[-\bar{Q}_L \cdot \tilde{\Phi}_i \eta_i^U U_R - \bar{Q}_L \cdot \Phi_i \eta_i^{D\dagger} D_R - \bar{L}_L \cdot \Phi_i \eta_i^{L\dagger} E_R + \text{h.c.} \Big] . \tag{40}$$

It is, however, more convenient to write it in the Higgs basis, where it similarly is

$$\begin{aligned} -\mathcal{L}_Y = {} & \bar{Q}_L \tilde{H}_1 \kappa^U U_R + \bar{Q}_L H_1 \kappa^{D\dagger} D_R + \bar{L}_L H_1 \kappa^{L\dagger} E_R \\ & + \bar{Q}_L \tilde{H}_2 \rho^U U_R + \bar{Q}_L H_2 \rho^{D\dagger} D_R + \bar{L}_L H_2 \rho^{L\dagger} E_R + \text{h.c.} . \end{aligned} \tag{41}$$

The Yukawa κ^F matrices are the diagonal mass matrices,

$$\kappa^U = \hat{v}_a^* \eta_a^U = \frac{\sqrt{2}}{v}\text{diag}(m_u, m_c, m_t),$$
$$\kappa^D = \hat{v}_a^* \eta_a^D = \frac{\sqrt{2}}{v}\text{diag}(m_d, m_s, m_b),$$
$$\kappa^L = \hat{v}_a^* \eta_a^L = \frac{\sqrt{2}}{v}\text{diag}(m_e, m_\mu, m_\tau). \tag{42}$$

Here, we have assumed a biunitary transformation of the right and left handed fermion fields such that the κ^F matrices are diagonal. It is in the general case impossible to diagonalize all the Yukawa matrices and $\rho^F = \hat{w}_a^* \eta_a^F$ are left as arbitrary complex 3×3 matrices.

In short, the scalar sector of the 2HDM contains several more scalar couplings as well as three new Yukawa matrices for the additional Higgs doublet, compared to the SM. In the general 2HDM, there is the possibility of explicit $\mathcal{CP}$ violation since the parameters ρ^F, m_{12}^2 and $\lambda_{5,6,7}$ are allowed to be complex.

3.3. Scalar kinetic mixing

When considering the general 2HDM, or any model with indistinguishable scalar fields, there is one step of diagonalizing the kinetic term that often is being overlooked. If one were to write down every gauge invariant term there is, one should also include the term

$$\mathcal{L} = \kappa \partial_\mu \Phi_1^\dagger \partial^\mu \Phi_2 + \text{h.c.} + \dots \tag{43}$$

in the Lagrangian from the start. There is good reason for not doing so, since it is well known that this kinetic mixing term can be diagonalized with a field redefinition at tree-level, as described in sec.12.5 of ref. [25]. However, things are not so trivial when dealing with loop corrections and the renormalization group. In the general 2HDM, there are infinites in the 2-point *Green functions*,

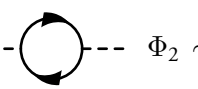

$$\sim \frac{1}{\epsilon}\text{Tr}(\eta_1^{F\dagger}\eta_2^F) + \dots \ . \tag{44}$$

For the diagonal case, these can be absorbed into the field strength renormalization of Φ_1 and Φ_2; however, one must also introduce a non-diagonal renormalization to absorb the ϵ pole in the non-diagonal diagrams simultaneously. In ref. [26], they regard the parameter κ as a parameter that must be renormalized and hence get a RGE of its own. There, the motivation is that since κ is being induced in the RG evolution, one cannot diagonalize the kinetic terms at all renormalization scales. But only physical parameters are in need

of renormalization and κ does not correspond to any such quantity. That the 2-point function is containing unphysical divergences is not a problem since 2-point functions do not correspond to physical quantities directly. They do, however, contain information about the physical masses of the theory.

To analyze the analytic structure of the 2-point function, we can make use of the *Källen-Lehmann spectral representation*. Taking the Fourier transform of the 2-point function of p^2 in the complex plane gives

$$G_{ij}(p^2) \equiv \int \mathrm{d}^4x e^{ipx} \langle\Omega| T(\Phi_i\Phi_j) |\Omega\rangle = \int_0^\infty \frac{\mathrm{d}M^2}{2\pi}\rho_{ij}(M^2)\frac{i}{p^2 - M^2 + i\epsilon}. \tag{45}$$

Although this is a general non-perturbative formula, we do not know the spectral density function $\rho_{ij}(M^2)$ from first principles. It should, however, contain isolated delta functions corresponding to single particle states[8]. In terms of matrix elements, it is

$$\rho_{ij}(M^2) = 2\pi\sum_k \delta(M^2 - m_k^2) \langle\Omega| \Phi_i(0) |m_k; \mathbf{p} = 0\rangle \langle m_k; \mathbf{p} = 0| \Phi_j |\Omega\rangle + \dots. \tag{46}$$

The masses m_k are the physical pole masses of the particles. Given that the scalar fields have the same quantum numbers, a particle state will in general have an overlap with all the scalar operators; meaning that all the components of ρ_{ij} are non-zero. Except for isolated single particle states, there are other contributions to the spectral density corresponding to bound states; which would occur at $M^2 \gtrsim (2m_k)^2$. However, near the single particle states, where the momentum goes on-shell, the 2-point function takes the form

$$G_{ij}(p^2) \to \frac{iZ_{ij}^{(k)}}{p^2 - m_k^2 + i\epsilon}, \qquad \text{as} \qquad p^2 \to m_k^2, \tag{47}$$

where the residue is parameterized by $Z_{ij}^{(k)}$, *i.e.*

$$Z_{ij}^{(k)} = -i \lim_{p^2\to m_k^2} (p^2 - m_k^2) G_{ij}(p^2). \tag{48}$$

Green functions are related to physical scattering amplitudes through the *Lehmann-Symanzik-Zimmermann theorem*. It takes general n-point Green functions and isolates scatterings of physical on-shell external particles to arrive at S-matrix elements. In a theory with non-diagonal 2-point functions, there are mixings on the legs as illustrated in figure 6. and thus

[8]For a proof of this, see the pololog section 10.2 in ref. [25].

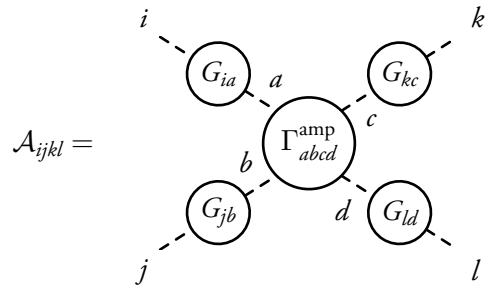

Figure 6: Scattering amplitude for scalar particles with non-diagonal 2-point functions. $\Gamma^{\text{amp}}_{abcd}$ is the amputated fully connected Green function.

the amplitude for 2-by-2 scalar scattering takes the form

$$\begin{aligned}\mathcal{A}_{ijkl} = \frac{1}{\sqrt{Z^{(i)}_{ii} Z^{(j)}_{jj} Z^{(k)}_{kk} Z^{(l)}_{ll}}} &\times \lim_{p_1^2 \to m_i^2} (p_1^2 - m_i^2) G_{ia}(p_1^2) \times \lim_{p_2^2 \to m_j^2} (p_2^2 - m_j^2) G_{jb}(p_2^2) \\ &\times \lim_{p_3^2 \to m_k^2} (p_3^2 - m_k^2) G_{kc}(p_3^2) \times \lim_{p_4^2 \to m_l^2} (p_4^2 - m_l^2) G_{ld}(p_4^2) \\ &\times \Gamma^{\text{amp}}_{abcd}(p_1, p_2, p_3, p_4), \end{aligned} \tag{49}$$

The key point of this discussion is that there is no need to introduce and renormalize parameters such as κ in eq. (43) in order to deal with infinities in non-diagonal 2-point functions. Even though the 2-point functions contain divergences, the physical quantities, like the scattering amplitude in eq. (49), are finite after renormalization; it is just a matter of picking a renormalization scheme. In eq. (49), all the infinities can be absorbed into the counter term for the 4-scalar interaction term.

This problem is further discussed in paper II, where we calculate the 1-loop RGEs in three different renormalization schemes for a toy model and explicitly show how all of the schemes are related through renormalization scale dependent field redefinitions.

This subtlety with scalar kinetic mixing is easy to overlook when deriving the RGEs. In the conventional scheme most often used in the literature, the kinetic mixing term is compensated for by having multidimensional anomalous dimensions for the scalar fields. The 2-loop RGEs for any renormalizable QFT in 4 dimensions were already derived in the 80s [5–7] and later extended to also include massive parameters as well as fixing some small errors in ref. [8]. Strictly speaking, the formulas presented there are written in an irreducible representation for the scalar fields, but they can be generalized somewhat straightforwardly to also be valid for theories with multiple indistinguishable scalar fields[9].

[9]The same issue is also discussed in ref. [27, 28].

3.4. Flavor-changing-neutral currents

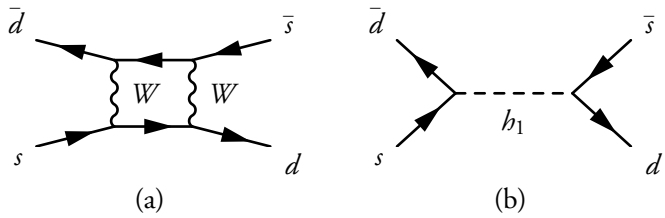

Figure 7: Contributions to neutral Kaon oscillation in the SM (a) and the general 2HDM (b) which exhibits FCNCs at tree-level.

There is one immediate problem with the general 2HDM: the presence of tree-level **Flavor-Changing-Neutral Currents** (FCNCs). For example, in the $\mathcal{CP}$ conserving 2HDM, the interaction of the lightest neutral $\mathcal{CP}$ even Higgs boson with down type quarks is

$$-\mathcal{L}_Y = \frac{1}{\sqrt{2}}\bar{D}\left[\kappa^D s_{\beta-\alpha} + (\rho^{D\dagger}P_R + \rho^D P_L)c_{\beta-\alpha}\right] D h_1, \tag{50}$$

where α is an angle arising from diagonalizing the $\mathcal{CP}$ even neutral Higgs mass matrix. Looking at eq. (50), it is evident that since ρ^F are arbitrary complex 3-by-3 matrices, the 2HDM exhibits non-diagonal couplings of fermions to neutral Higgs bosons. As mentioned previously, these FCNCs arise because one cannot diagonalize all the Yukawa matrices with a biunitary transformation of the fermion fields like one does in the SM. Such tree-level couplings are absent in the SM and gives rise to processes that otherwise are loop suppressed. For example, neutral Kaon meson oscillation is a process that occurs at the 1-loop level in the SM. In the general 2HDM, this process receives contributions at tree-level, see figure 7, from the interactions in eq. (50). Since the SM is in agreement with experiments, these FCNCs must be severely suppressed for the model not to be ruled out.

A popular solution to get rid of the tree-level FCNCs is to impose a discrete symmetry on the model. The simplest symmetry is a $\mathbb{Z}_2$ one [29, 30], where one Higgs doublet is even and the other is odd. There are four different choices one can make for the right handed fermion fields under the $\mathbb{Z}_2$ symmetry as listed in table 1. The effect is that the up type quarks only acquire masses from one Higgs doublet; similarly for the down type quarks and leptons. Then, it is possible to diagonalize all the matrices and ρ^F becomes proportional to κ^F as in table 1. This effectively gets rid of three Yukawa matrices.

Imposing a $\mathbb{Z}_2$ symmetry also forbids the m_{12}^2 and $\lambda_{6,7}$ parameters in the potential; making λ_5 the only potentially complex parameter. However, one always has the freedom to absorb one phase into the fields with a Higgs flavor basis transformation, which consequently makes the $\mathbb{Z}_2$ symmetric 2HDM also $\mathcal{CP}$ conserving.

Table 1: Different $\mathbb{Z}_2$ symmetries that can be imposed on the 2HDM. Φ_1 is odd(-1) and Φ_2 is even$(+1)$. For every type of $\mathbb{Z}_2$ symmetry, the ρ^F matrices become proportional to the diagonal mass matrices, $\rho^F = a^F \kappa^F$.

Type	U_R	D_R	L_R	a^U	a^D	a^L
I	+	+	+	$\cot\beta$	$\cot\beta$	$\cot\beta$
II	+	−	−	$\cot\beta$	$-\tan\beta$	$-\tan\beta$
Y	+	−	+	$\cot\beta$	$-\tan\beta$	$\cot\beta$
X	+	+	−	$\cot\beta$	$\cot\beta$	$-\tan\beta$

3.5. Electric dipole moment and flavor physics

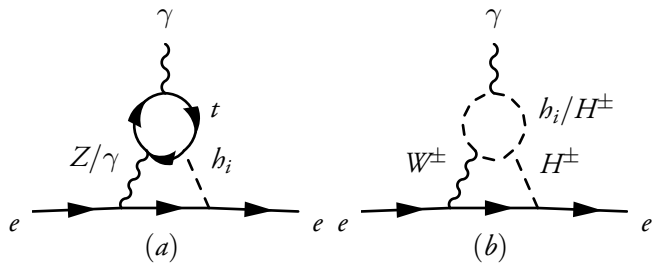

Figure 8: Typical Barr-Zee diagrams in the 2HDM that contribute to the electric dipole moment of the electron. In (a) there are also diagrams with $W^\pm$ or $H^\pm$ instead of the fermion loop. In (b) there is an additional fermion loop diagram as well that contributes if the Yukawa sector is not $\mathbb{Z}_2$ symmetric.

One way to explain the cosmic baryon asymmetry of the universe is through electroweak baryogenesis [31–33]. However, to fulfill Sakharov's criteria for baryogenesis [34], one needs a strong first order phase transition and a source of $\mathcal{CP}$ violation for this to work and the SM fails on both account. The Higgs boson mass is too high for a first order phase transition [35,36] and the amount of $\mathcal{CP}$ violation in the CKM matrix is too low [37–39]. The 2HDM can be a remedy for electroweak baryogenesis, since it exhibits the possibility of a first order phase transition [40], while also offering new sources of $\mathcal{CP}$ violation. It is thus interesting to investigate how large the $\mathcal{CP}$ violation can be. The new sources cannot be arbitrarily large because of severe constraints coming from electric dipole moments. Currently there is no direct evidence for a non-zero electric dipole moment for any fundamental particle and the task of measuring one is a challenging problem. Still, there exist upper limits that are easily violated in the 2HDM. The cleanest particle to probe to date is the electron and, recently, the ACMEII collaboration [41] placed a new bound on the electric dipole moment of the electron to be

$$|d_e| < 1.1 \times 10^{-29} \text{ e cm}, \tag{51}$$

using a system of ThO molecules. Even though the SM predicts a non-zero d_e, it is many orders of magnitude lower than the current bound. But the 2HDM, with complex parameters, can easily produce d_e in the range of 10^{-26} to 10^{-30} e cm; making it vital to check the parameter points. The largest contribution to d_e comes from 2-loop Barr-Zee diagrams [42] as the ones shown in figure 8.

There are many other observables that can be used to constrain the parameter space of the 2HDM. Of course, there are the direct searches of new scalar particles at colliders, but the extra Higgs particles can also influence calculations in flavor physics that are in agreement with the SM. For example, the charged Higgs boson interacts with quarks through

$$-\mathcal{L}_Y = \bar{U}\left(V_{CKM}\rho^{D\dagger}P_R - \rho^{U\dagger}V_{CKM}P_L\right)DH^+ + \text{h.c.}\,. \tag{52}$$

Thus, the charged Higgs contributes to the process $b \to s\gamma$ through so called penguin diagrams, shown in figure 9. As a consequence, weak radiative B-meson decays put a lower bound on the mass of the charged Higgs boson [43–47]. If one has a type I $\mathbb{Z}_2$ symmetry there is a $\tan\beta$ dependent bound when $\tan\beta \lesssim 2$; while with a type II $\mathbb{Z}_2$ symmetry one gets the conservative bound $m_{H^\pm} \gtrsim 580$ GeV [47]. We do not apply these limits in our studies of the 2HDM, but one should keep in mind that they exist.

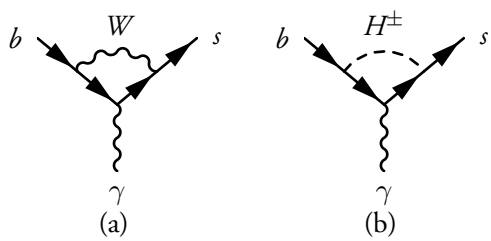

Figure 9: Diagrams for $b \to s\gamma$ in the SM (a) and the general 2HDM (b).

3.6. Breaking the symmetry

Since the exact $\mathbb{Z}_2$ symmetry is a very constraining requirement, one often breaks the symmetry *softly* by allowing for $m_{12}^2 \neq 0$. This softly broken $\mathbb{Z}_2$ symmetric 2HDM is by far the most studied scenario, *e.g.* the 2HDM as the effective theory of the minimal supersymmetric SM is of such a type at tree-level. Having a non-zero m_{12}^2 is regarded as soft breaking since the consequences are not that bad; it induces no symmetry breaking Yukawa interactions. If one breaks the symmetry *hard*, by having $\lambda_{6,7} \neq 0$ or a non-symmetric Yukawa

sector, the results are quite different. One phenomenon that arises is that the symmetry breaking spreads under RG evolution. The soft breaking mass term m_{12}^2 does not enter the massless parameters' RGEs, while the opposite is not true. Thus a small hard breaking of the $\mathbb{Z}_2$ symmetry can generate more symmetry breaking during the RG evolution of the 2HDM. Moreover, the symmetry breaking can spread across the sectors, *e.g.* a flavor conserving Yukawa sector at one scale might get FCNCs at another scale if $\lambda_{6,7} \neq 0$.

At 1-loop order, the Yukawa sector's RGEs are independent of the scalar quartic couplings. Therefore, one has to employ 2-loop RGEs for the 2HDM to fully see how the symmetry breaking spreads throughout all sectors. It is a central goal of both papers III and V to give a quantitative answer to how much the hard breaking spreads during RG evolution in the $\mathcal{CP}$ conserving and violating scenarios respectively.

3.7. Renormalization group evolution

"A man's got to have a code."

Omar, The Wire

Generalizing the results of ref. [8], we derived the 2-loop RGEs for the general complex 2HDM. Since these are very long, we omit writing them out in this thesis. The RGEs are practically impossible to solve analytically and, in the end, their usage is mainly to perform numerical calculations. Since deriving the 2-loop RGEs and writing code to perform the RG evolution is a tedious and error prone task, we developed the public code `2HDME` that is described in paper IV. It can perform the RG evolution of the 2HDM and the interested reader can find the RGEs in the source code.

When investigating the parameter space of the 2HDM we make sure to only consider parameter points that are not excluded by collider data. Out of the four Higgs bosons, one of them has to resemble the 125 GeV signal at the LHC, while the others must not violate any exclusion bounds coming from collider searches. We make use of `HiggsBounds` [48–50] and `HiggsSignals` [51] to implement these constraints. `HiggsBounds` determines if a certain parameter point is allowed or excluded by comparing to experimental cross section limits coming from LEP, Tevatron and LHC. `HiggsSignals` performs a statistical χ^2 fit to the measurements of the 125 GeV signal. All these codes require the calculations of decay widths and rates for all Higgs bosons, for which we use a modified version of `2HDMC` [52]; that is extended to also be valid for the complex $\mathcal{CP}$ violating 2HDM.

In the work of papers III and V, we investigate the RG effects of breaking the $\mathbb{Z}_2$ symmetry at one particular scale. As already hinted in section 2.3, there is a wealth of information in the RG evolution of a model. The 2HDM exhibits a large parameter space with substantial freedom in choosing a physical scenario. By being able to evolve the 2HDM in

renormalization scale one has a powerful tool to investigate how stable specific parameter configurations are at *e.g.* the electroweak scale. At some energy scale in the evolution, the model might break down which would point to the need of new physics for the specific scenario. The RG evolution results can then give a hint of any fine tuning in the choice of parameters.

There are several consistency checks of the 2HDM that can be performed to make sure that one deals with a "good" model. One such constraint is to require unitarity of the scattering matrix of scalar particles at high energies; effectively putting an upper bound on the quartic couplings. Another theoretical constraint is to make sure that one is in a stable global minimum of the potential; or at least in a metastable minimum with a lifetime greater than the age of the universe. Finally, one immediately runs into trouble during the RG evolution if one hits a Landau pole as explained in section 2.3. In such a case, all parameters goes to infinity since the RGEs form a coupled system of equations. Near the pole, perturbation theory breaks down and one would either need some new physics to remedy this or the theory becomes strongly coupled.

All these consistency checks are implemented at tree-level in `2HDME`. In the numerical evolutions, the presence of Landau poles is implemented as a tree-level perturbativity constraint; meaning a simple higher bound on the parameters in the Lagrangian.

With these tools at hand, paper III and V analyze the parameter space of 2HDM. Among the results are quantitative measures of how large FCNCs, as well as $\lambda_{6,7}$, can be generated in cases with a broken $\mathbb{Z}_2$ symmetry. Also, what parameter regions contain consistent models all the way up to the Planck scale. Paper III deals solely with the $\mathcal{CP}$ conserved 2HDM, while paper V completes the study by allowing for $\mathcal{CP}$ violation. In $\mathcal{CP}$ violating scenarios, complex phases also spread during RG running. To constrain the amount of $\mathcal{CP}$ violation we calculate the electron's EDM, by summing up all of the relevant Barr-Zee diagrams. The focus of the study is to provide the general characteristics of RG running in the 2HDM. Furthermore, the effects studied here should be similar in other multi scalar models.

4. Soft-Collinear-Effective Theory

In section 3, we introduced the 2HDM as a proposed extension of the SM. The 2HDM contains the SM in a certain decoupling limit; *e.g.* when the BSM scalar particles are much heavier than the lightest one. Any deviation of the 125 GeV scalar particle from the SM's characteristics would be of immense importance. While experimentalists gather more data, a lot of work is being done to calculate all the observables that are being measured at the LHC to ever increasing accuracies. An example of such an observable that can be calculated analytically is the transverse momentum spectrum of the Higgs boson; which is the focus of attention in paper I. However, before we actually get to this calculation, we first take a few steps back and introduce the concept of effective field theories as well as the framework of SCET.

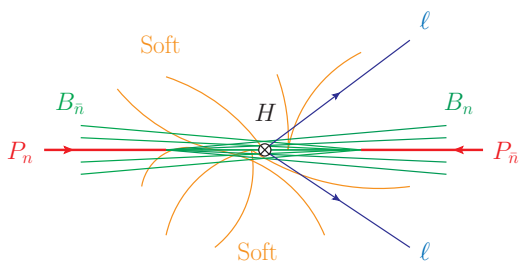

Figure 10: A typical hadron collision with a lepton-pair final state. Each P_n denotes an incoming proton along the directions n^μ and $\bar{n}^\mu$. In SCET, these are described by beam functions, B_n, that contain all the collinear radiation along the corresponding beam axis. The soft radiation is described by the soft function. There is also a hard function denoted as H for the hard interaction in the process.

In hadron colliders, such as LHC, a good understanding and description of the phenomena arising from the strong force is absolutely necessary. Collimated collections of particles in the form of jets are ubiquitous. The very thing that is being accelerated - the proton - is itself a soup of quarks and gluons and the resulting collision event is bound to be messy. All these processes have all different characteristic energy scales which is a further complication. At energy scales below Λ_{QCD}, the quarks and gluons are interacting strongly rendering only non-perturbative techniques applicable. On the opposite end, two partons in the collision will make up a hard process that will have $s \approx m_h^2$; for Higgs production. All the particles will also emit additional particles that have momentum components in the entire energy range. It is vital to disentangle all these processes to make any calculation possible. A typical proton collision is shown in figure 10, where the collinear radiation along the beam axis is

colored green, while the soft radiation in all directions is orange. SCET disentangles these different types of radiation at the level of the Lagrangian.

Originally, SCET was developed in the field of low-energy quantum chromodynamics; in particular B-meson flavor physics [53–58]. Now, there are plenty of applications of SCET to high-energy collider physics as well and in this section we will only briefly sketch out the basics of the framework. For a more detailed summary of SCET, see the review in ref. [59] or chap.36 of the introductory textbook in ref. [60].

4.1. Effective Field Theories

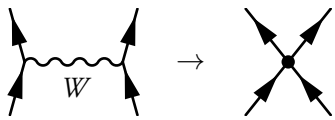

(53)

Figure 11: Integrating out the W boson yields a low energy EFT.

In previous sections, we have introduced the concept of how RGEs describe a theory's change in behavior when probing another length scale. When the change in behavior is more dramatic and one passes thresholds where certain degrees of freedom cease to be dynamic ones, it is more illuminating and easier to construct a so called *Effective Field Theory* (EFT). For example, a particular model can contain a particle that is too massive to be excited as a dynamical degree of freedom in the low energy regime. Then, one talks about "integrating out" the particle which yields an EFT. In the path integral formalism, we can sketch the process as

$$Z[J] = \int \mathcal{D}\phi_{\text{light}} \mathcal{D}\phi_{\text{heavy}} e^{iS[\phi_{\text{light}}, \phi_{\text{heavy}}]} = \int \mathcal{D}\phi_{\text{light}} e^{iS_{\text{EFT}}[\phi_{\text{light}}]}, \tag{54}$$

where S_{EFT} is the action of the EFT, which then has an energy regime of validity ranging up to roughly the mass of the heavy particle that was integrated out.

A classic example of an EFT in particle physics is the one that emerges due to integrating out the W boson. Since the W boson is relatively heavy at around 80 GeV, it is not created as a real on-shell particle in low energy processes. One can then simplify all internal W propagators by expanding in momentum like

$$\frac{-i\left(g^{\mu\nu} - p^\mu p^\nu / m_W^2\right)}{p^2 - m_W^2} = \frac{-ig^{\mu\nu}}{m_W^2} + \mathcal{O}\left(p^2/m_W^4\right). \tag{55}$$

This yields a low energy EFT that is valid for $p^2 \ll m_W^2$. The EFT will then contain non-renormalizable 4-fermion operators as illustrated in figure 11; where the propagator is

simply collapsing to a single point. As an example, muon decay is precisely such a process where one can employ this EFT.

4.2. Momenta regions and power expansion

A proper EFT should contain a power counting parameter $\lambda \ll 1$. In the example in section 4.1, of integrating out the W, this would correspond to m_W^{-2}. SCET does not integrate out full particles but rather divides the participating particles of a collision into different regions depending on the scaling of their momenta. If one considers the radiation off a highly energetic particle it can take two forms: the particle can split into collinear particles along the same trajectory; or there is a soft particle emission at a wider angle.

It is very convenient to work in light-cone coordinates when dealing with high energy particles with a small invariant mass. In such a system one substitutes the time axis and one space axis for the light-cone boundary axes. Using the light-like reference vectors $n^\mu = (1,0,0,1)$ and $\bar{n}^\mu = (1,0,0,-1)$, any four vector can be decomposed as

$$p^\mu = (n\cdot p)\frac{\bar{n}^\mu}{2} + (\bar{n}\cdot p)\frac{n^\mu}{2} + p_\perp^\mu \equiv p_+^\mu + p_-^\mu + p_\perp^\mu : (p_+, p_-, p_\perp). \tag{56}$$

For the sake of simplicity we will discuss the specific observable of interest in paper I: *the transverse momentum spectrum of Higgs production in proton collisions*. Even more specifically, we will only deal with the phase space region of small transverse momentum compared to the hard interaction scale, $\Lambda_{\text{QCD}}^2 \ll \mathbf{p}_\perp^2 \ll m_h^2$, and we will thus set the power expansion parameter to be $\lambda = |\mathbf{p}_\perp|/m_h$.

This region of small transverse momentum is suffering from large double logarithms of the form $\log^2(m_h^2/\mathbf{p}_\perp^2)$. These cause fixed order perturbation theory to break down just as in section 2.2. Therefore, it is essential to resum these logarithmic terms.

Table 2: The momenta scaling modes in light-cone coordinates.

Four-momenta	Invariant mass	Mode
$p_h^\mu \sim m_h(1,1,\lambda)$	$p^2 \sim m_h^2$	hard
$p_n^\mu \sim m_h(\lambda^2,1,\lambda)$	$p^2 \sim m_h^2\lambda^2$	n-collinear
$p_{\bar{n}}^\mu \sim m_h(1,\lambda^2,\lambda)$	$p^2 \sim m_h^2\lambda^2$	$\bar{n}$-collinear
$p_s^\mu \sim m_h(\lambda,\lambda,\lambda)$	$p^2 \sim m_h^2\lambda^2$	soft

Using light-cone coordinates, the produced Higgs boson will have a momentum that scales as $p^\mu \sim m_h(1,1,\lambda)$. Any radiation that recoils against such a state will have a similar $\mathbf{p}_\perp$ scaling. The relevant scaling modes in light-cone coordinates are listed in table 2. While the hard modes have an invariant mass of $\mathcal{O}\left(m_h^2\right)$, both the soft and collinear modes live on the same invariant mass hyperbola in the $\{p^+, p^-\}$ plane as sketched out in figure 12.

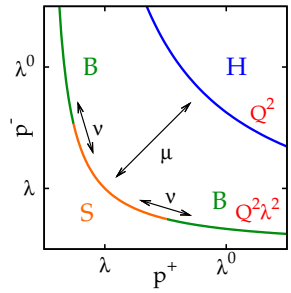

Figure 12: The characteristic energy scales for the light-cone momentum components for the hard, beam and soft sectors. The invariant mass is set by $p^- p^+$; hence, they all lie on a hyperbola. The fact that the beam and soft functions lie on the same hyperbola, gives rise to rapidity divergences.

4.3. The SCET ingredients

Traditional QCD computations containing multiple energy scales resort to a diagrammatic expansion such as the method of regions. But with such a method, disentangling the contributions coming from each phase space region is increasingly difficult when going to higher orders in perturbation theory. SCET is formulated already with a proper power counting at the level of the Lagrangian. This allows for a systematic organization of the power corrections, i.e. the higher order terms in the expansion parameter λ. It also makes it easier to ensure features such as gauge invariance; which is not manifest on the level of individual diagrams. However, in the end, the diagrams of SCET will be in one-to-one correspondence with the QCD expanded ones.

To properly construct SCET is a complicated procedure that will not be covered in detail in this thesis. In short, one splits up the quark and gluon fields in separate collinear and soft fields,

$$q(x) = \chi_n(x) + \chi_{\bar{n}}(x) + \chi_s(x) + \dots, \quad A_\mu(x) = A^n_\mu(x) + A^{\bar{n}}_\mu(x) + A^s_\mu(x) + \dots, \tag{57}$$

where every field excitation then has a definite momentum scaling. The Lagrangian will in the end be a sum of collinear and soft sectors,

$$\mathcal{L} = \mathcal{L}_n + \mathcal{L}_{\bar{n}} + \mathcal{L}_s + \dots, \tag{58}$$

which allows for a factorization of particle states in matrix elements.

4.4. Collinear-soft interactions

Although we will not go through the derivation of the SCET Lagrangian, we will work backwards and motivate the final results by looking at the soft-collinear limit of QCD.

Hard fluctuations are integrated out and appear in Wilson coefficients of the EFT operators. In SCET, one can perform a systematic counting of powers of λ to see what should be included. The interaction of soft gluon fields with collinear quark fields is of order λ^0 and one must include an infinite number of soft gluon emissions from the collinear particles. However, the soft limit of QCD is simple in that for every soft emission one gets an *eikonal factor* to the matrix element. Taking the simplest example of some process with an external quark, we define the matrix element as

$\bar{u}(p)\mathcal{M}(p) \equiv$ 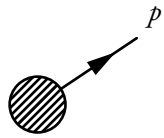 . (59)

Now, say the external quark is emitting a soft gluon with momentum k. In the soft emission limit one can expand the intermediate quark propagator, which yields the result

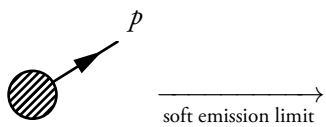

$$= -g_3 \bar{u}(p) t^a \frac{p \cdot \epsilon}{p \cdot k} \mathcal{M}(p), \tag{60}$$

where t^a is a group factor of $SU(3)_c$. The same expression of the soft emission limit can be reproduced by introducing path ordered Wilson lines,

$$S_n^\dagger(x) = \mathbf{P} \exp\left[i g_3 \int_0^\infty \mathrm{d}s \; n \cdot A(x + sn) e^{-\varepsilon s} \right]. \tag{61}$$

Evaluating the matrix element with a soft gluon gives

$$\begin{aligned} \langle k | \, S_n^\dagger(0) \, | \Omega \rangle &= i g_3 \int_0^\infty \mathrm{d}s \; e^{-\varepsilon s} \langle k | \, n \cdot A(sn) \, | \Omega \rangle + \mathcal{O}(g_3^2) \\ &\approx i g_3 n \cdot \epsilon t^a \int_0^\infty \mathrm{d}s \; e^{i(k \cdot n + i\varepsilon)s} \\ &= \left(\frac{-g_3 n \cdot \epsilon t^a}{n \cdot k + i\varepsilon} \right), \end{aligned} \tag{62}$$

where we used

$$\langle k|\, A^a_\mu(x) t^a \,|\Omega\rangle = e^{ik\cdot x}\epsilon_\mu(k) t^a. \tag{63}$$

Although the formulas get more cumbersome, the above matrix element reproduces the soft limit of an arbitrary number of soft gluons; one simply expands the Wilson line to higher order in g_3. All the interactions of soft gluons with the energetic quarks can be described completely by introducing one Wilson line for every quark. In the end, the matrix element factorizes as

$$\begin{aligned}\langle p_1, \ldots; k_1, \ldots k_m|\, \bar{q}_n \cdots q_n \,|\ldots, p_n\rangle \xrightarrow[\text{soft emission limit}]{} &\langle p_1, \ldots|\, \bar{q}_n \cdots q_n \,|\ldots, p_n\rangle \\ &\times \langle k_1, \ldots, k_m|\, S^\dagger_{n_1} \cdots S_{n_n} \,|\Omega\rangle\,.\end{aligned} \tag{64}$$

This factorization is useful, since one then can calculate the effect of soft radiation by purely computing the vacuum matrix element of Wilson lines. Such matrix elements are referred to as *soft functions*.

4.5. Factorization and soft function

With the framework of SCET in place, one can factorize the cross section into a hard, two beam and a soft function. Schematically, we write it as

$$\frac{d\sigma}{d^2\mathbf{p}_\perp} \sim H(m_h) \times B(\mathbf{p}_\perp) \otimes_\perp B(\mathbf{p}_\perp) \otimes_\perp S(\mathbf{p}_\perp). \tag{65}$$

The soft-collinear emissions recoil against the Higgs boson and thus have a combined transverse momentum in the opposite direction. This manifests itself in the differential cross section as a convolution in the transverse momentum. All the soft interactions are moved into the soft function, which is similar to the one sketched out in previous section, but now contains a measurement delta function for the transverse momentum. The explicit soft function for quarks going into the hard interaction is

$$S^q(\mathbf{p}_\perp) = \frac{1}{N_c}\langle\Omega|\,\mathrm{Tr}\left\{\bar{T}\left[S^\dagger_n S_{\bar{n}}\right]\delta^{(2)}(\mathbf{p}_\perp - \mathcal{P}_\perp)\, T\left[S^\dagger_{\bar{n}} S_n\right]\right\}|\Omega\rangle\,, \tag{66}$$

where $\mathcal{P}_\perp$ is a projection operator that picks up the transverse momentum of the real emissions and $N_c = 3$ for QCD. To compute the soft function, one expands the Wilson lines. At 1-loop order, there is only one kind of diagram contributing, which is displayed in figure 2. All 2-loop diagrams are shown in paper I.

To recap: Although very sketchy, we have described the process of factorizing a cross section into separate functions. The soft function only depends on the number of incoming and

outgoing colored states. It does not depend on the internal collinear radiation of those beam or jet functions. In this way, both the soft and the beam functions are process independent and only depend on whether one matches onto a quark or gluon current going into the hard interaction.

4.6. Resummation and rapidity divergences

When calculating the loop diagrams in the hard, beam and soft functions one encounters the normal infrared and ultraviolet divergences that are regulated with dimensional regularization and manifests themselves as poles as $1/\epsilon$. In the end these will cancel out in the renormalization procedure. There is, however, additional divergences that show up after factorizing the cross section as in eq. (65) that are neither infrared nor ultraviolet in nature. These so called *rapidity divergences* are a consequence of the factorization.

These rapidity divergences are related to integrals of the form:

$$I = \int_{|\mathbf{p}_\perp|}^{m_h} \frac{\mathrm{d}p^+}{p^+} = \log(m_h/|\mathbf{p}_\perp|), \tag{67}$$

which range over both the soft and collinear limits. In the factorization process, the resulting soft and collinear sectors share the same invariant mass scaling, see figure 12. The integral above is split up with a cut-off, Λ, as

$$I = \int_{|\mathbf{p}_\perp|}^{\Lambda} \frac{\mathrm{d}p^+}{p^+} + \int_{\Lambda}^{m_h} \frac{\mathrm{d}p^+}{p^+} \to \int_{|\mathbf{p}_\perp|}^{\infty} \frac{\mathrm{d}p^+}{p^+} + \int_{0}^{m_h} \frac{\mathrm{d}p^+}{p^+}, \tag{68}$$

which is taken[10] to ∞ or 0. In the calculation, there is only one scale dependence for these logarithms in each sector, but taking the cut-off limits introduces divergences that need to be regulated. In paper I, we use the framework of ref. [61, 62] that uses a regulator which effectively inserts factors of

$$\left(\frac{\nu}{|k^- - k^+|}\right)^\eta \tag{69}$$

in the loop integrals. The divergences show up as $1/\eta$ poles and cancel when combining the beam and soft functions. The ν parameter is a dimensionful renormalization scale similar to μ in dimensional regularization. In the end, the renormalized soft function will be μ

[10] That Λ is taken to different limits is similar to cancelling infrared and ultraviolet divergences in dimensional regularization, *i.e.* that $\frac{1}{\epsilon_{IR}} - \frac{1}{\epsilon_{UV}} = 0$.

and ν dependent and will obey both a RGE as well as a **Rapidity RGE** (RRGE),

$$\mu \frac{\mathrm{d}}{\mathrm{d}\mu} S(\mu,\nu) = \gamma_{S,\mu}(\mu,\nu)\, S(\mu,\nu)\,, \tag{70}$$

$$\nu \frac{\mathrm{d}}{\mathrm{d}\nu} S(\mu,\nu) = \gamma_{S,\nu}(\mu)\, S(\mu,\nu)\,. \tag{71}$$

There is a huge benefit of splitting up the integrals as above. Then every sector only depends on a single scale and one can effectively minimize all integrals by a suitable renormalization scale choice. The scenario is a little bit more complicated because of the presence of double logarithms of the form $\log^2(m_b^2/\mathbf{p}_\perp^2)$. The factorization of the cross section effectively splits up these logarithms into

$$\begin{aligned}\log^2 \frac{m_b^2}{\mathbf{p}_\perp^2} &= \log^2 \frac{m_b^2}{\mu^2} + 2 \log \frac{m_b^2}{\mu^2} \log \frac{\mu^2}{\mathbf{p}_\perp^2} + \log^2 \frac{\mu^2}{\mathbf{p}_\perp^2} \\ &= \log^2 \frac{m_b^2}{\mu^2} + 2 \left(\log \frac{m_b^2}{\nu^2} + \log \frac{\nu^2}{\mu^2} \right) \log \frac{\mu^2}{\mathbf{p}_\perp^2} + \log^2 \frac{\mu^2}{\mathbf{p}_\perp^2},\end{aligned} \tag{72}$$

where μ is the usual renormalization scale in dimensional regularization. After the factorization the different logarithms are contained in different sectors and the logarithms can be minimized with some renormalization scale choice; that is different for every function as illustrated in figure 13. Then one must run each function using RGEs and RRGEs to a common point in the renormalization scale space. Evolving each function corresponds to resumming all the logarithms. Of course the final expression for the cross section is independent of the final renormalization or rapidity scale.

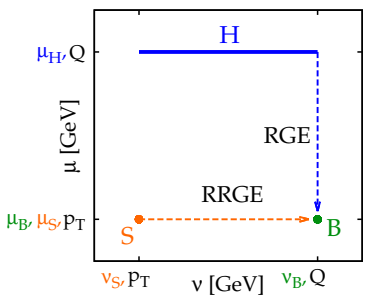

Figure 13: Renormalization and rapidity scale space. The hard, beam and soft functions have different characteristic energy scales associated with each μ and ν. To minimize all the logarithms, one uses RGEs and RRGEs to run them to an arbitrary common point.

The 2-loop anomalous dimensions $\gamma_{S,\mu(\nu)}$ in eqs.70 and 71 are some of the main results of paper I. The main benefit of this framework of introducing a rapidity scale and RRGE is

that one can achieve a better estimate of the theoretical uncertainty in the resummation of logarithms by varying both the renormalization and rapidity scale independently of one another.

5. Final words

"One must imagine Sisyphus happy."
Albert Camus, The Myth of Sisyphus

After the Higgs particle discovery, no one knows what is next in the field of particle physics. With the LHC working full time to probe the high energy frontier, people are waiting for the results to come in. Perhaps is new physics just around the corner or maybe there is nothing new that will be discovered at the current generation of accelerators.

What is certain, is that the current experiments will test the SM intensely. Precision calculations will be essential when looking for anomalies. In this introduction, we have gone over the techniques of employing the renormalization group to perform resummation, but also how to use it when investigating models beyond the SM. Hopefully, the interested reader will now be more ready to continue reading the following publications.

6. Overview of the papers

Below is a short summary of each paper in this thesis together with a description of my contributions. The author list of each paper is ordered alphabetically.

Paper I: Rapidity renormalized TMD soft and beam functions at two loops

Thomas Lübbert, Joel Oredsson and Maximilian Stahlhofen.
e-print: arXiv:1602.01829 [hep-ph]. *JHEP*, 03 (2016) 168.

This paper concerns the analytic calculation of the transverse momentum spectrum of a heavy color-neutral final state in proton collisions using SCET. In the low $\vec{p}_T$ region, this observable suffers from large logarithms that need to be resummed. Furthermore, the factorization of the cross section into hard, beam and soft functions gives rise to so-called rapidity divergences that are not regulated with dimensional regularization.

Our main result is the calculation of the soft function to NNLO using the rapidity regulator of ref. [61, 62]. Using this scheme, we derive RGEs as well as Rapidity RGEs (RRGE) for the separate functions in the cross section; that then can be used for resumming all the large logarithms. An advantage of the RRGE is that one can systematically study the perturbative uncertainties by independent variations of all the factorization/renormalization scales.

With the full NNLO soft function at our disposal, we also derive the NNLO beam functions in the same RRG scheme by comparing to the results of ref. [63, 64]; thus making all ingredients available for NNLL' resummation.

This project is based on the work I did during my master thesis at DESY, Hamburg. The project was suggested by Frank Tackmann; who also supervised the majority of the project in the beginning. All the analytical calculations were performed by me with extensive help from Thomas Lübbert and Maximilian Stahlhofen. Thomas Lübbert also cross checked a lot of the results. I wrote the first draft of the paper, which was then improved and extended by the others.

Paper II: Kinetic mixing

Johan Bijnens, Joel Oredsson, Johan Rathsman.
e-print: arXiv:1810.04483 [hep-ph]. *Phys.Lett.*, B792 (2019) 238-243.

In theories with multiple scalar fields that have equal quantum numbers, there is the possibility to include a kinetic mixing term in the Lagrangian,

$$\mathcal{L} = \kappa(\partial_\mu \phi_1)(\partial^\mu \phi_2) + \dots \,. \tag{73}$$

Although it is well known that such a term can be removed by diagonalizing the kinetic terms with a field redefinition, it was claimed in ref. [26, 65] that the parameter κ needs to be included when performing a RGE analysis.

The main goal of this paper is to show that this is not necessary since κ is not a physical parameter; it all depends on the renormalization scheme if one should include scalar kinetic mixing or not. To show this, we perform a 1-loop calculation of the RGEs in a toy model using three different renormalization schemes: one with scalar kinetic mixing; one that only renormalizes physical observables; and the standard scheme. We also derive the renormalization scale dependent transformations that relate each of these schemes to one another.

This is also relevant when using the formalism in ref. [5–8] for deriving 2-loop RGEs. They express their formulas in an irreducible representation of the scalar fields and one must be

careful and generalize their results in theories with scalar fields that mix under RG evolution. This has also been discussed independently by ref. [27, 28].

This paper started off as a side project when me and Johan Rathsman worked on deriving the general 2-loop RGEs for the 2HDM for paper III. It was during that process, that we discovered subtleties and confusion in the literature when it came to RGEs for theories with multiple identical scalar fields. Johan Bijnens then joined the project and came up with the idea of a pedagogical example using three renormalization schemes. I and Johan Bijnens performed the calculations independently and he also wrote the first draft; which was later improved and extended by me and subsequently Johan Rathsman.

Paper III: $\mathbb{Z}_2$ breaking effects in 2-loop RG evolution of 2HDM

Joel Oredsson, Johan Rathsman.
e-print: arXiv:1810.02588 [hep-ph]. *JHEP*, 02 (2019) 152.

This paper studies how a small breaking of a $\mathbb{Z}_2$ symmetry spreads in the RG evolution of the general $\mathcal{CP}$ conserved 2HDMs. Since the Yukawa sector is independent of the scalar sector at 1-loop order, one has to work with 2-loop RGEs to see any effects of the symmetry breaking spreading across the Yukawa and scalar sectors.

In order to do this analysis, we first derived the general 2-loop RGEs for the 2HDM using the general formalism in ref. [5–8]. To perform the RG evolution, we created a `C++` code that numerically solves the RGEs; which grew into the open-source program `2HDME` described in paper IV. For doing experimental checks of parameter points, we also implemented an interface to `HiggsBounds` and `HiggsSignals`.

Using `2HDME`, we perform some parameter scans of four scenarios with different kinds of $\mathbb{Z}_2$ symmetry. Then we performed a bottom-up RG evolution, where we checked for violation of tree-level unitarity or stability as well as the emergence of Landau poles.

The idea for this project was Johan Rathsman's, who also provided constant help and guidance throughout the process. I performed all the analytical derivations of the 2-loop RGEs. The code was written by me, but some parts are inspired by the code `2HDMC` [52]; which Johan Rathsman is a coauthor of. I also wrote the paper, with Johan Rathsman providing corrections and improvements.

Paper IV: 2 Higgs Doublet Model Evolver - Manual

Joel Oredsson.
e-print: arXiv:1811.08215 [hep-ph]. *CPC* 2019.05.021.

This paper is a manual for the open-source code `2HDME`. The code performs the RG evolution of the general, potentially $\mathcal{CP}$ violating, 2HDM using 2-loop RGEs. It does so by solving a system of 129 coupled ordinary differential equations numerically. Furthermore, calculations of the oblique parameters S, T and U, as well as simple tree-level tests of perturbativity, unitarity and stability are implemented. The manual goes through the structure of the code and contains instructions for how to use it.

This project is a documentation of the code that I developed as a tool for performing the analysis in paper III. The manual is written by me, but Johan Rathsman provided helpful corrections, suggestions and comments.

Paper V: 2-loop RG evolution of $\mathcal{CP}$ violating 2HDM

Joel Oredsson, Johan Rathsman.
e-print: arXiv:1909.05735 [hep-ph]. *Submitted to JHEP.*

This is an extension of our previous work in paper III. While paper III focuses solely on the $\mathcal{CP}$ conserving 2HDM, we here allow for $\mathcal{CP}$ violation. We similarly investigate RG effects in the 2HDM and especially the consequences of having a small $\mathbb{Z}_2$ symmetry breaking. In the $\mathcal{CP}$ violating scenario, one also gets phases that spread during RG evolution. To constrain the amount of $\mathcal{CP}$ violation, we implement a calculation of the electron's EDM in our code.

I have performed all the programming, created the plots and written the paper with constant guidance from Johan Rathsman; who also corrected, as well as, provided suggestions and improvements to the manuscript.

Bibliography

[1] **Particle Data Group** Collaboration, M. Tanabashi *et al.*, "Review of Particle Physics," *Phys. Rev.* **D98** no. 3, (2018) 030001.

[2] D. Hanneke, S. Fogwell, and G. Gabrielse, "New Measurement of the Electron Magnetic Moment and the Fine Structure Constant," *Phys. Rev. Lett.* **100** (2008) 120801, arXiv:0801.1134 [physics.atom-ph].

[3] D. Hanneke, S. F. Hoogerheide, and G. Gabrielse, "Cavity Control of a Single-Electron Quantum Cyclotron: Measuring the Electron Magnetic Moment," *Phys. Rev.* **A83** (2011) 052122, arXiv:1009.4831 [physics.atom-ph].

[4] T. Aoyama, M. Hayakawa, T. Kinoshita, and M. Nio, "Tenth-Order Electron Anomalous Magnetic Moment — Contribution of Diagrams without Closed Lepton Loops," *Phys. Rev.* **D91** no. 3, (2015) 033006, arXiv:1412.8284 [hep-ph]. [Erratum: Phys. Rev.D96,no.1,019901(2017)].

[5] M. E. Machacek and M. T. Vaughn, "Two Loop Renormalization Group Equations in a General Quantum Field Theory. 1. Wave Function Renormalization," *Nucl. Phys.* **B222** (1983) 83–103.

[6] M. E. Machacek and M. T. Vaughn, "Two Loop Renormalization Group Equations in a General Quantum Field Theory. 2. Yukawa Couplings," *Nucl. Phys.* **B236** (1984) 221–232.

[7] M. E. Machacek and M. T. Vaughn, "Two Loop Renormalization Group Equations in a General Quantum Field Theory. 3. Scalar Quartic Couplings," *Nucl. Phys.* **B249** (1985) 70–92.

[8] M.-x. Luo, H.-w. Wang, and Y. Xiao, "Two loop renormalization group equations in general gauge field theories," *Phys. Rev.* **D67** (2003) 065019, arXiv:hep-ph/0211440 [hep-ph].

[9] J. Oredsson, "2 Higgs Doublet Model Evolver - Manual," arXiv:1811.08215 [hep-ph]. https://github.com/jojelen/2HDME.

[10] **ATLAS** Collaboration, G. Aad *et al.*, "Observation of a new particle in the search for the Standard Model Higgs boson with the ATLAS detector at the LHC," *Phys. Lett.* **B716** (2012) 1–29, arXiv:1207.7214 [hep-ex].

[11] **CMS** Collaboration, S. Chatrchyan *et al.*, "Observation of a new boson at a mass of 125 GeV with the CMS experiment at the LHC," *Phys. Lett.* **B716** (2012) 30–61, arXiv:1207.7235 [hep-ex].

[12] **ATLAS, CMS** Collaboration, G. Aad *et al.*, "Measurements of the Higgs boson production and decay rates and constraints on its couplings from a combined ATLAS and CMS analysis of the LHC pp collision data at $\sqrt{s} = 7$ and 8 TeV," *JHEP* **08** (2016) 045, arXiv:1606.02266 [hep-ex].

[13] P. Langacker, "Grand Unified Theories and Proton Decay," *Phys. Rept.* **72** (1981) 185.

[14] T. D. Lee, "A Theory of Spontaneous T Violation," *Phys. Rev.* **D8** (1973) 1226–1239. [,516(1973)].

[15] H. E. Haber and G. L. Kane, "The Search for Supersymmetry: Probing Physics Beyond the Standard Model," *Phys. Rept.* **117** (1985) 75–263.

[16] S. P. Martin, "A Supersymmetry primer," arXiv:hep-ph/9709356 [hep-ph]. [Adv. Ser. Direct. High Energy Phys.18,1(1998)].

[17] R. D. Peccei and H. R. Quinn, "CP Conservation in the Presence of Instantons," *Phys. Rev. Lett.* **38** (1977) 1440–1443. [,328(1977)].

[18] J. E. Kim, "Light Pseudoscalars, Particle Physics and Cosmology," *Phys. Rept.* **150** (1987) 1–177.

[19] G. Branco, P. Ferreira, L. Lavoura, M. Rebelo, M. Sher, *et al.*, "Theory and phenomenology of two-Higgs-doublet models," *Phys.Rept.* **516** (2012) 1–102, arXiv:1106.0034 [hep-ph].

[20] J. de Blas *et al.*, "Higgs Boson Studies at Future Particle Colliders," arXiv:1905.03764 [hep-ph].

[21] S. Davidson and H. E. Haber, "Basis-independent methods for the two-Higgs-doublet model," *Phys. Rev.* **D72** (2005) 035004, arXiv:hep-ph/0504050 [hep-ph]. [Erratum: Phys. Rev.D72,099902(2005)].

[22] H. E. Haber and D. O'Neil, "Basis-independent methods for the two-Higgs-doublet model. II. The Significance of tanβ," *Phys. Rev.* **D74** (2006) 015018, arXiv:hep-ph/0602242 [hep-ph]. [Erratum: Phys. Rev.D74,no.5,059905(2006)].

[23] H. E. Haber and D. O'Neil, "Basis-independent methods for the two-Higgs-doublet model III: The CP-conserving limit, custodial symmetry, and the oblique parameters S, T, U," *Phys. Rev.* **D83** (2011) 055017, arXiv:1011.6188 [hep-ph].

[24] G. C. Branco, L. Lavoura, and J. P. Silva, "CP Violation," *Int. Ser. Monogr. Phys.* **103** (1999) 1–536.

[25] S. Weinberg, *The Quantum theory of fields. Vol. 1: Foundations*. Cambridge University Press, 2005.

[26] I. F. Ginzburg, "Necessity of mixed kinetic term in the description of general system with identical scalar fields," *Phys. Lett.* **B682** (2009) 61–66, arXiv:0810.1546 [hep-ph].

[27] I. Schienbein, F. Staub, T. Steudtner, and K. Svirina, "Revisiting RGEs for general gauge theories," arXiv:1809.06797 [hep-ph].

[28] A. V. Bednyakov, "On Three-loop RGE for the Higgs Sector of 2HDM," arXiv:1809.04527 [hep-ph].

[29] S. L. Glashow and S. Weinberg, "Natural Conservation Laws for Neutral Currents," *Phys. Rev.* **D15** (1977) 1958.

[30] E. A. Paschos, "Diagonal Neutral Currents," *Phys. Rev.* **D15** (1977) 1966.

[31] V. A. Kuzmin, V. A. Rubakov, and M. E. Shaposhnikov, "On the Anomalous Electroweak Baryon Number Nonconservation in the Early Universe," *Phys. Lett.* **155B** (1985) 36.

[32] M. E. Shaposhnikov, "Possible Appearance of the Baryon Asymmetry of the Universe in an Electroweak Theory," *JETP Lett.* **44** (1986) 465–468. [Pisma Zh. Eksp. Teor. Fiz.44,364(1986)].

[33] M. E. Shaposhnikov, "Baryon Asymmetry of the Universe in Standard Electroweak Theory," *Nucl. Phys.* **B287** (1987) 757–775.

[34] A. D. Sakharov, "Violation of CP Invariance, C asymmetry, and baryon asymmetry of the universe," *Pisma Zh. Eksp. Teor. Fiz.* **5** (1967) 32–35. [Usp. Fiz. Nauk161,no.5,61(1991)].

[35] A. I. Bochkarev and M. E. Shaposhnikov, "Electroweak Production of Baryon Asymmetry and Upper Bounds on the Higgs and Top Masses," *Mod. Phys. Lett.* **A2** (1987) 417.

[36] K. Kajantie, M. Laine, K. Rummukainen, and M. E. Shaposhnikov, "The Electroweak phase transition: A Nonperturbative analysis," *Nucl. Phys.* **B466** (1996) 189–258, arXiv:hep-lat/9510020 [hep-lat].

[37] M. B. Gavela, P. Hernandez, J. Orloff, and O. Pene, "Standard model CP violation and baryon asymmetry," *Mod. Phys. Lett.* **A9** (1994) 795–810, arXiv:hep-ph/9312215 [hep-ph].

[38] P. Huet and E. Sather, "Electroweak baryogenesis and standard model CP violation," *Phys. Rev.* **D51** (1995) 379–394, arXiv:hep-ph/9404302 [hep-ph].

[39] M. B. Gavela, P. Hernandez, J. Orloff, O. Pene, and C. Quimbay, "Standard model CP violation and baryon asymmetry. Part 2: Finite temperature," *Nucl. Phys.* **B430** (1994) 382–426, arXiv:hep-ph/9406289 [hep-ph].

[40] P. Basler, M. Krause, M. Muhlleitner, J. Wittbrodt, and A. Wlotzka, "Strong First Order Electroweak Phase Transition in the CP-Conserving 2HDM Revisited," *JHEP* **02** (2017) 121, arXiv:1612.04086 [hep-ph].

[41] **ACME** Collaboration, V. Andreev *et al.*, "Improved limit on the electric dipole moment of the electron," *Nature* **562** no. 7727, (2018) 355–360.

[42] S. M. Barr and A. Zee, "Electric Dipole Moment of the Electron and of the Neutron," *Phys. Rev. Lett.* **65** (1990) 21–24. [Erratum: Phys. Rev. Lett.65,2920(1990)].

[43] O. Deschamps, S. Descotes-Genon, S. Monteil, V. Niess, S. T'Jampens, and V. Tisserand, "The Two Higgs Doublet of Type II facing flavour physics data," *Phys. Rev.* **D82** (2010) 073012, arXiv:0907.5135 [hep-ph].

[44] F. Mahmoudi and O. Stal, "Flavor constraints on the two-Higgs-doublet model with general Yukawa couplings," *Phys. Rev.* **D81** (2010) 035016, arXiv:0907.1791 [hep-ph].

[45] T. Hermann, M. Misiak, and M. Steinhauser, "$\bar{B} \to X_s\gamma$ in the Two Higgs Doublet Model up to Next-to-Next-to-Leading Order in QCD," *JHEP* **11** (2012) 036, arXiv:1208.2788 [hep-ph].

[46] M. Misiak *et al.*, "Updated NNLO QCD predictions for the weak radiative B-meson decays," *Phys. Rev. Lett.* **114** no. 22, (2015) 221801, arXiv:1503.01789 [hep-ph].

[47] M. Misiak and M. Steinhauser, "Weak radiative decays of the B meson and bounds on $M_{H^\pm}$ in the Two-Higgs-Doublet Model," *Eur. Phys. J.* **C77** no. 3, (2017) 201, arXiv:1702.04571 [hep-ph].

[48] P. Bechtle, O. Brein, S. Heinemeyer, G. Weiglein, and K. E. Williams, "HiggsBounds: Confronting Arbitrary Higgs Sectors with Exclusion Bounds from LEP and the Tevatron," *Comput. Phys. Commun.* **181** (2010) 138–167, arXiv:0811.4169 [hep-ph].

[49] P. Bechtle, O. Brein, S. Heinemeyer, G. Weiglein, and K. E. Williams, "HiggsBounds 2.0.0: Confronting Neutral and Charged Higgs Sector Predictions with Exclusion Bounds from LEP and the Tevatron," *Comput. Phys. Commun.* **182** (2011) 2605–2631, arXiv:1102.1898 [hep-ph].

[50] P. Bechtle, O. Brein, S. Heinemeyer, O. Stål, T. Stefaniak, G. Weiglein, and K. E. Williams, "HiggsBounds – 4: Improved Tests of Extended Higgs Sectors against Exclusion Bounds from LEP, the Tevatron and the LHC," *Eur. Phys. J.* **C74** no. 3, (2014) 2693, arXiv:1311.0055 [hep-ph].

[51] P. Bechtle, S. Heinemeyer, O. Stål, T. Stefaniak, and G. Weiglein, "*HiggsSignals*: Confronting arbitrary Higgs sectors with measurements at the Tevatron and the LHC," *Eur. Phys. J.* **C74** no. 2, (2014) 2711, arXiv:1305.1933 [hep-ph].

[52] D. Eriksson, J. Rathsman, and O. Stål, "2HDMC: Two-Higgs-Doublet Model Calculator Physics and Manual," *Comput. Phys. Commun.* **181** (2010) 189–205, arXiv:0902.0851 [hep-ph].

[53] C. W. Bauer, S. Fleming, D. Pirjol, and I. W. Stewart, "An Effective field theory for collinear and soft gluons: Heavy to light decays," *Phys.Rev.* **D63** (2001) 114020, arXiv:hep-ph/0011336 [hep-ph].

[54] C. W. Bauer, S. Fleming, and M. E. Luke, "Summing Sudakov logarithms in $B \to X_s\gamma$ in effective field theory," *Phys. Rev. D* **63** (2000) 014006, arXiv:hep-ph/0005275 [hep-ph].

[55] C. W. Bauer and I. W. Stewart, "Invariant operators in collinear effective theory," *Phys.Lett.* **B516** (2001) 134–142, arXiv:hep-ph/0107001 [hep-ph].

[56] C. W. Bauer, D. Pirjol, and I. W. Stewart, "Soft collinear factorization in effective field theory," *Phys.Rev.* **D65** (2002) 054022, arXiv:hep-ph/0109045 [hep-ph].

[57] C. W. Bauer, D. Pirjol, and I. W. Stewart, "Factorization and endpoint singularities in heavy to light decays," *Phys. Rev.* **D67** (2003) 071502, arXiv:hep-ph/0211069 [hep-ph].

[58] M. Beneke, A. P. Chapovsky, M. Diehl, and T. Feldmann, "Soft collinear effective theory and heavy to light currents beyond leading power," *Nucl. Phys.* **B643** (2002) 431–476, arXiv:hep-ph/0206152 [hep-ph].

[59] T. Becher, A. Broggio, and A. Ferroglia, "Introduction to Soft-Collinear Effective Theory," *Lect. Notes Phys.* **896** (2015) pp.1–206, arXiv:1410.1892 [hep-ph].

[60] M. D. Schwartz, *Quantum Field Theory and the Standard Model*. Cambridge University Press, 2014. http://www.cambridge.org/us/academic/subjects/physics/theoretical-physics-and-mathematical-physics/quantum-field-theory-and-standard-model.

[61] J.-y. Chiu, A. Jain, D. Neill, and I. Z. Rothstein, "The Rapidity Renormalization Group," *Phys.Rev.Lett.* **108** (2012) 151601, arXiv:1104.0881 [hep-ph].

[62] J.-Y. Chiu, A. Jain, D. Neill, and I. Z. Rothstein, "A Formalism for the Systematic Treatment of Rapidity Logarithms in Quantum Field Theory," *JHEP* **1205** (2012) 084, arXiv:1202.0814 [hep-ph].

[63] T. Gehrmann, T. Lübbert, and L. L. Yang, "Transverse parton distribution functions at next-to-next-to-leading order: the quark-to-quark case," *Phys. Rev. Lett.* **109** (2012) 242003, arXiv:1209.0682 [hep-ph].

[64] T. Gehrmann, T. Lübbert, and L. L. Yang, "Calculation of the transverse parton distribution functions at next-to-next-to-leading order," *JHEP* **1406** (2014) 155, arXiv:1403.6451 [hep-ph].

[65] I. F. Ginzburg and M. Krawczyk, "Symmetries of two Higgs doublet model and CP violation," *Phys. Rev.* **D72** (2005) 115013, arXiv:hep-ph/0408011 [hep-ph].

Printed by Media-Tryck, Lund 2019 NORDIC SWAN ECOLABEL 3041 0903

LUND UNIVERSITY

Department of Astronomy and Theoretical Physics
Faculty of Science
Lund University
ISBN 978-91-7895-255-7